Supplementary Information

Efficient organic solar cells based on low-cost pentacyclic fused-ring small molecule acceptors with a fill factor over 80%

Qingya Wei,*[a] Yuanyuan Li,[b] Weikun Chen,[b] Qinhao Shi,[b] Shaofeng Zhu,[b] Wensheng Yan*[a] and Yingping Zou*[b]

[a]Institute of Carbon Neutrality and New Energy, School of Electronics and Information, Hangzhou Dianzi University, Hangzhou 310018, PR China

[b]State Key Laboratory of Powder Metallurgy, College of Chemistry and Chemical Engineering, Central South University, Changsha 410083, China

*Corresponding authors

E-mail: qingyawei@hdu.edu.cn; wensheng.yan@hdu.edu.cn; yingpingzou@csu.edu.cn

Contents

1. Materials and Measurements

All chemicals and reagents, unless otherwise specified, were purchased from Energy Chemical, Innochem or other commercial resources and were used without further purification. PM6 was purchased from Solarmer Energy Inc. The synthesis of BZ4F-ch1 and BZ4F-ch2 is similar to that of BZ4F except preparing the dialdehyde compound[1]. Compound 4 and compound 10 were synthesized according to the reported literature[1].

^{1}H NMR and ^{13}C NMR spectra were recorded using a Bruker AV-400 spectrometer in a deuterated chloroform solution at 298 K, unless specified otherwise. Chemical shifts are reported as δ values (ppm) with tetramethylsilane (TMS) as the internal reference. The molecular mass was confirmed using an Autoflex III matrix-assisted laser desorption ionization mass spectrometer (MALDI-TOF-MS). Thermogravimetric analysis (TGA) was conducted on a Perkin-Elmer TGA-7 with a heating rate of 10 K/min under nitrogen. UV-Vis absorption spectra were recorded on the SHIMADZU UV-2600 spectrophotometer. The cyclic voltammetry results were obtained with a computer-controlled CHI 660E electrochemical workstation.

The morphologies of the PM6/acceptor blend films were investigated by atomic force microscopy (AFM, Agilent Technologies, 5500 AFM/SPM System, USA) in contacting mode with a 5 μm scanner. Transmission electron microscopy (TEM) measurements were performed in a JEM-2100F. Samples for the TEM measurements were prepared as following: The active layer films were spin-casted on ITO/ PEDOT:PSS substrates, and the substrates with active layers were submerged in deionized water to make the active layers floats onto the air-water interface. Then, the floated films were picked upon an unsupported 200 mesh copper grids for the TEM measurements. The density functional theory (DFT) was measured by the Gauss software package on B3LYP/6-31G* level.

2. Fabrications and Characterization of OSCs

The optimized solar cell devices were fabricated with a conventional structure of Glass/ITO/PEDOT: PSS (40 nm)/PM6: acceptor/PDINN (5nm)/Ag. Pre-patterned ITO coated glass substrates (purchased from Advanced Election Technology Co., Ltd) were washed with deionized water and isopropyl alcohol in an ultrasonic bath for 15 minutes each. After blow-drying by high-purity nitrogen, all ITO substrates are cleaned in the ultraviolet ozone cleaning system for 15 minutes. Subsequently, a thin layer of PEDOT: PSS (Xi'an Polymer Light Technology Corp 4083) was deposited through spin-coating on pre-cleaned ITO-coated glass at 5000 rpm for 40 s and dried subsequently at 150°C for 15 minutes in atmospheric air. Then the photovoltaic layers were spin-coated in a glovebox from a solution of PM6:BZ4F-ch1 and PM6:BZ4F-ch2 (16 mg/mL with 10 mg/mL 1,3,5-trichlorobenzene (TCB)), with the PM6/acceptor weight ratio of 1:1.2 in chloroform. The optimal active layers were fabricated by spin-coating at about 3200 rpm for the 30s. Then the PM6:BZ4F-ch1 and PM6:BZ4F-ch2 films were treated with thermal annealing at 90℃ for 10 min. After cooling to room temperature, a PDINN layer via a solution concentration of 1 mg/mL was deposited at the top of the active layer at a rate of 3000 rpm for 30 s. Finally, the top Ag electrode of 100 nm thickness was thermally evaporated through a mask onto the cathode buffer layer under a vacuum of 1.5×10^{-4} mbar. The thickness of optimal active layers measured by a Bruker Dektak XT stylus profilometer were about 100 nm. Current density–voltage (*J–V*) curves of the devices were performed by a Keithley 2400 source meter in a glove box with a nitrogen atmosphere. The simulated sunlight was calibrated by an AM 1.5G solar simulator (Enlitech, SS-F5, Taiwan), which was measured with a calibrated Si diode from National Renewable Energy Laboratory. The EQE curves were tested by an EnLi Technology (Taiwan) EQE measurement system. The typical effective area of the device is 0.0484 cm^2.

Electron mobility and hole mobility measurements:

The electron mobility device adopted the ITO/ZnO/active layer/PDINN/Ag structure,

and the hole mobility device adopted the ITO/PEDOT: PSS/active layer/MoO_3/Ag structure. The electron and hole mobilities were calculated according to the space charge limited current (SCLC) method by the equation: $J = 9\mu\varepsilon_r\varepsilon_0 V^2/8d^3$, where J was the current density, μ is the electron or hole mobility, V is the internal voltage in the device, ε_r is the relative dielectric constant of active layer material, ε_0 is the permittivity of empty space, and d is the thickness of the active layer.

TPV/TPC measurements

TPV measurement was conducted under 1 sun conditions by illuminating the device with a white light-emitting diode, and the champion device was set to the open-circuit condition. For TPC measurement, the champion device was set to the short-circuit condition in dark. The output signal was collected by key sight oscilloscope. Voltages at open circuit and currents under short circuit conditions were measured over a 1 MΩ and a 50 Ω resistor, respectively.

3. General synthetic procedures of the acceptors

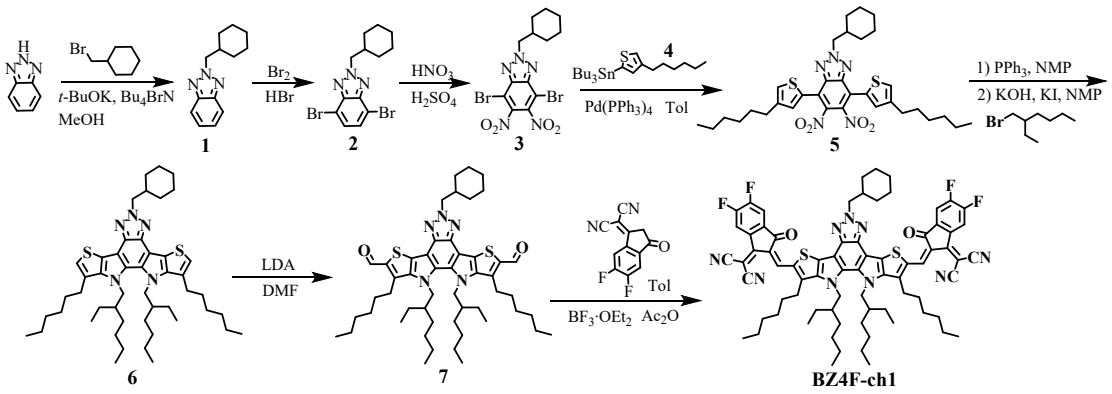

Scheme S1. Synthetic procedure of BZ4F-ch1.

Synthesis of 2-(cyclohexylmethyl)-2*H*-benzo[*d*][1,2,3]triazole (1)

2*H*-benzo[*d*][1,2,3]triazole (20 g, 167.88 mmol), a potassium tert-butoxide (*t*-BuOK, 19.78 g, 176.27 mmol) solution in methanol (200 mL), (bromomethyl)cyclohexane (35.67 g, 201.46 mmol) and tetrabutylammonium bromide

(1 g) were added to a three-necked flask, and then heated to 90 °C for 24 h. The reaction mixture was then cooled to room temperature, poured into water (200 mL), and extracted with dichloromethane for three times. The organic layer was collected and dried with anhydrous $MgSO_4$, residual solvent was removed under reduced pressure, and the residue was purified by silica gel chromatography with petroleum ether/dichloromethane (4:1, v/v) eluent to obtain compound 1 as a colorless liquid. (18.07 g, 50% yield). ^{1}H NMR (400 MHz, Chloroform-*d*) δ 7.86 (dd, *J* = 6.5, 3.1 Hz, 2H), 7.37 (dd, *J* = 6.6, 3.1 Hz, 2H), 4.56 (d, *J* = 7.3 Hz, 2H), 2.21 (dtp, *J* = 14.5, 7.1, 3.5 Hz, 1H), 1.75 – 1.58 (m, 5H), 1.30 – 1.03 (m, 5H).

Synthesis of 4,7-dibromo-2-(cyclohexylmethyl)-2*H*-benzo[*d*][1,2,3]triazole (2)

Compound 1 (10 g, 46.45 mmol) and hydrobromic acid (HBr, 100 mL) were added to a three-necked flask and stirred for 30 min at 100 °C, then a liquid bromine (Br_2, 6.54 g, 127.74 mmol) solution in HBr (20 mL) was added dropwise to the reaction mixture. After 10 h, the mixture was cooled to room temperature and poured into ice water (300 mL). Sodium thiosulfate ($Na_2S_2O_3$) was used to remove the residual Br_2. The mixture was extracted with dichloromethane for three times. The organic layer was collected and dried with anhydrous $MgSO_4$, residual solvent was removed under reduced pressure, and the residue was purified by silica gel chromatography with petroleum ether/dichloromethane (4:1, v/v) eluent to obtain compound 2 as a white solid. (14.21 g, 82% yield). ^{1}H NMR (400 MHz, Chloroform-*d*) δ 7.44 (s, 2H), 4.61 (d, *J* = 7.4 Hz, 2H), 2.26 (dtp, *J* = 14.0, 6.9, 3.4, 3.0 Hz, 1H), 1.74 – 1.56 (m, 5H), 1.18 (ddt, *J* = 53.5, 21.5, 10.7 Hz, 5H).

Synthesis of 4,7-dibromo-2-(cyclohexylmethyl)-5,6-dinitro-2*H*-benzo[*d*][1,2,3] triazole (3)

The concentrated nitric acid (HNO_3, 65%, 42 g) was added dropwise to concentrated sulfuric acid (H_2SO_4, 98%, 172 g) at 0 °C, and stirred for 30 min. Compound 2 (8 g, 21.44 mmol) was then added to the mixed acid in batches and stirred for another 5 h at ambient temperature. The mixture was poured into ice water (300 mL). Sodium

hydrogen carbonate ($NaHCO_3$) was used to remove the residual Br_2. The mixture was extracted with dichloromethane for three times. The organic layer was collected and dried with anhydrous $MgSO_4$, residual solvent was removed under reduced pressure, and the compound 3 was purified by silica gel chromatography with petroleum ether/dichloromethane (4:1, v/v) eluent as a white solid. (9.14 g, 92% yield). ^{1}H NMR (400 MHz, Chloroform-*d*) δ 4.69 (d, *J* = 7.3 Hz, 2H), 2.26 (dtq, *J* = 14.5, 7.0, 3.6 Hz, 1H), 1.75 – 1.61 (m, 5H), 1.31 – 1.09 (m, 5H).

Synthesis of 2-(cyclohexylmethyl)-4,7-bis(4-hexylthiophen-2-yl)-5,6-dinitro-2*H*-benzo[*d*][1,2,3]triazole (5)

Compound 3 (2.06 g, 4.45 mmol), compound 4 (5.1 g, 11.13 mmol) and Pd $(PPh_3)_4$ (0.26 g, 0.22 mmol) were dissolved in toluene (30mL) and stirred at 75℃ for 4h under argon atmosphere. The solvent was removed under vacuum after the reaction mixture was cooled to ambient temperature. Compound 5 was purified by chromatography in a silica gel column eluting with hexanes/dichloromethane (2:1, v/v) as a brown-red oil. (2.44 g, 86% yield). ^{1}H NMR (400 MHz, Chloroform-*d*) δ 7.32 (s, 2H), 7.25 (s, 2H), 4.65 (d, *J* = 7.2 Hz, 2H), 2.65 (t, *J* = 7.7 Hz, 4H), 2.21 (dddq, *J* = 14.7, 10.7, 7.0, 3.6 Hz, 1H), 1.77 – 1.61 (m, 8H), 1.37 – 1.07 (m, 18H), 0.90 (t, *J* = 6.6 Hz, 6H).

Synthesis of 5-(cyclohexylmethyl)-10,11-bis(2-ethylhexyl)-1,9-dihexyl-10,11-dihydro-5*H*-thieno[2',3':4,5]pyrrolo[3,2-*g*]thieno[3,2-*b*][1,2,3]triazolo[4,5-*e*]indole (6)

Under argon, compound 5 (1.31 g, 2.06 mmol) and triphenylphosphine (5.4 g, 20.6 mmol) were dissolved in N-Methylpyrrolidone (NMP, 10 mL). The mixture was stirred at 180℃ overnight. After cooled to ambient temperature, to the mixture was added potassium hydroxide (1.15 g, 20.6 mmol), potassium iodide (82 mg,0.49 mmol) and 1-bromo-2-ethylhexane (3.97 g, 20.6 mmol). The mixture was stirred at 90℃ overnight under argon atmosphere. The organic layer was washed with water and brine and dried with $MgSO_4$. Compound 6 was obtained by column chromatography in a silica gel column eluting with hexanes/dichloromethane (4:1, v/v) as a tawny oil (0.90 g, 55%

yield). ^{1}H NMR (400 MHz, Chloroform-*d*) δ 6.98 (s, 2H), 4.62 (d, *J* = 7.3 Hz, 2H), 4.45 (d, *J* = 7.4 Hz, 4H), 2.90 (t, *J* = 7.5 Hz, 4H), 2.36 – 2.29 (m, 1H), 1.91 – 1.80 (m, 4H), 1.77 – 1.64 (m, 6H), 1.49 – 1.13 (m, 30H), 1.03 – 0.62 (m, 22H).

Synthesis of 5-(cyclohexylmethyl)-10,11-bis(2-ethylhexyl)-1,9-dihexyl-10,11-dihydro-5*H*-thieno[2',3':4,5]pyrrolo[3,2-*g*]thieno[3,2-*b*][1,2,3]triazolo[4,5-*e*]indole-2,8-dicarbaldehyde (7)

Under argon, LDA (2 mol L^{-1}, 9.1 mmol) was added dropwise into a solution of compound 6 (0.73 g, 0.91 mmol) in dry THF (15mL) at -78℃. The mixture was then stirred for 1h. Dry DMF (5 mL) was added, after string at -78℃ for another 30 min, the mixture was warmed to room temperature and reacted overnight. The mixture was poured into water (200 mL) and extracted with DCM. The organic layer was washed with water, dried by $MgSO_4$. Removing the solvent and the crude product was purified by column chromatography in a silica gel column, eluting with petroleum ether/dichloromethane (1:1, v/v) to give compound 7 as an orange solid. (0.68 g, 88% yield). ^{1}H NMR (400 MHz, Chloroform-*d*) δ 10.14 (s, 2H), 4.64 (d, *J* = 7.3 Hz, 2H), 4.47 (d, *J* = 6.0 Hz, 4H), 3.48 (s, 2H), 3.06 (s, 2H), 2.38 – 2.26 (m, 1H), 1.99 – 1.79 (m, 4H), 1.72 (dd, *J* = 22.1, 11.7 Hz, 6H), 1.53 – 0.99 (m, 30H), 0.95 – 0.28 (m, 22H).

Synthesis of 2,2'-((2Z,2'Z)-((5-(cyclohexylmethyl)-10,11-bis(2-ethylhexyl)-1,9-dihexyl-10,11-dihydro-5*H*-thieno[2',3':4,5]pyrrolo[3,2-g]thieno[3,2-*b*][1,2,3]triazolo[4,5-*e*]indole-2,8-diyl)bis(methaneylylidene))bis(5,6-difluoro-3-oxo-2,3-dihydro-1*H*-indene-2,1-diylidene))dimalononitrile (BZ4F-ch1)

Under argon, compound 7 (0.19 g, 0.22 mmol) and 2-(5,6-difluoro-3-oxo-2,3-dihydro-1H-inden-1-ylidene)malononitrile (123 mg, 0.53 mmol) were dissolved in toluene (10 mL). To the mixture boron trifluoride etherate (BF_3·OEt_2, 0.5 mL) and acetic anhydride (0.5 mL) were added. After stirring at room temperature for 0.5 h, the mixture was poured into methanol and filtered. The residue was purified in a silica gel column using petroleum ether/dichloromethane (1:2, v/v) as the eluent. BZ4F-ch1 was obtained as a black solid powder (261 mg, 93% yield). ^{1}H NMR (400 MHz, Chloroform-*d*) δ 9.21 (s,

2H), 8.57 (dd, *J* = 10.0, 6.5 Hz, 2H), 7.72 (t, *J* = 7.5 Hz, 2H), 4.65 (d, *J* = 7.3 Hz, 2H), 4.51 (s, 4H), 3.64 – 3.40 (m, 2H), 3.29 – 3.04 (m, 2H), 2.38 (ddt, *J* = 14.0, 6.6, 3.2 Hz, 1H), 2.02 – 1.60 (m, 12H), 1.54 – 1.45 (m, 4H), 1.42 – 1.02 (m, 22H), 0.89 (t, *J* = 6.8 Hz, 12H), 0.52 (dd, *J* = 40.5, 15.0 Hz, 6H), 0.27 – 0.11 (m, 6H). ^{13}C NMR (101 MHz, Chloroform-*d*) δ 185.83, 159.45, 143.78, 136.15, 136.07, 135.72, 134.62, 120.41, 115.30, 115.03, 114.81, 114.75, 112.64, 112.46, 112.28, 68.17, 62.58, 53.09, 39.04, 31.99, 31.80, 30.72, 30.14, 29.16, 28.41, 28.03, 26.29, 25.65, 23.77, 22.97, 22.51, 21.72, 14.13, 14.09, 13.88, 13.39, 11.02, 8.02. MALDI-TOF MS: calcd for $C_{75}H_{79}F_4N_9O_2S_2$ (M^+), 1277.5734; found, 1277.5704.

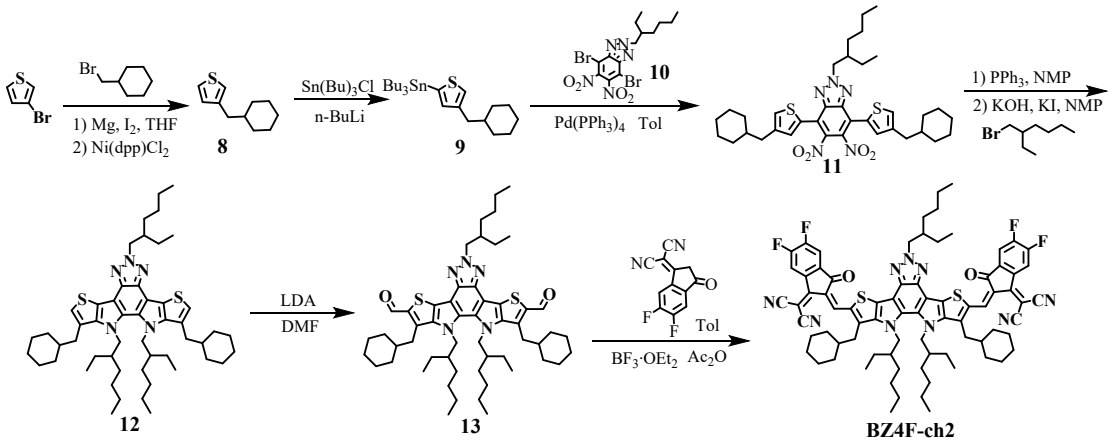

Scheme S2. Synthetic procedure of BZ4F-ch2.

Synthesis of 3-(cyclohexylmethyl)thiophene (8)

Magnesium powder (Mg, 1.07 g, 43.9 mmol) and iodine grains (I_2, 2-4 grains) were added to a three-necked flask (250 mL), to the flask a solution of (bromomethyl)cyclohexane (7.07 g, 39.91 mmol) in THF (40 mL) was dropped slowly under the protection of argon. The reaction was stirred at a slow speed, and the addition of (bromomethyl)cyclohexane was intermitted when the Mg/I_2 was soaked in THF. Meanwhile, the mixture was heated by blower. A red smog was then emerged, accompanied with bubbles. Subsequently, the (bromomethyl)cyclohexane was continued to be added into the reaction with the constant heating for 10 min. The reaction was stirred at 60 °C for another 3 h to obtain the gray Grignard reagent. Under argon, the newly prepared Grignard reagent was added dropwise to the mixture of 3-bromothiophene (5 g, 30.7 mmol), [1,3-Bis(diphenylphosphino)propane]nickel(II)

chloride ($NiCl_2$(dppp), 0.322 g, 0.614 mmol) in THF (20 mL) at 0 °C. Then, the reaction mixture was heated to 60 °C and stirred for 16 h. The mixture was cooled to room temperature, and the excess Mg was filtered. The filtrate was extracted with dichloromethane and water for three times. The organic layer was collected and dried with anhydrous $MgSO_4$, residual solvent was removed under reduced pressure, and the compound 8 was purified by silica gel chromatography with petroleum ether eluent as a colorless liquid. (2.94 g, 53% yield). ^{1}H NMR (400 MHz, Chloroform-*d*) δ 7.23 (dd, *J* = 4.8, 3.0 Hz, 1H), 6.90 (dd, *J* = 6.0, 3.9 Hz, 2H), 2.51 (d, *J* = 7.1 Hz, 2H), 1.69 (d, *J* = 11.1 Hz, 4H), 1.50 (ddt, *J* = 14.8, 7.3, 3.7 Hz, 1H), 1.26 – 1.13 (m, 4H), 0.97 – 0.87 (m, 2H).

Synthesis of tributyl(4-(cyclohexylmethyl)thiophen-2-yl)stannane (9)

Under argon atmosphere to a solution of compound 8 (3 g, 16.64 mmol) in THF (10 mL) was added n-BuLi (2.5 M, 18.3 mmol) at -78 ℃ over 30 min. Then the mixture was stirred for 1 h at the same temperature. Tributylchlorostannane (5.75 mL, 19.97 mmol) was added, and stirring at room temperature overnight. The mixture was quenched with water and extracted with petroleum ether. The crude product of compound 2 was obtained and directly used for the next step.

Synthesis of 4,7-bis(4-(cyclohexylmethyl)thiophen-2-yl)-2-(2-ethylhexyl)-5,6-dinitro-2*H*-benzo[*d*][1,2,3]triazole (11)

Compound 9 (7.81 g, 16.64 mmol), compound 10 (3.19 g, 6.66 mmol) and Pd $(PPh_3)_4$ (0.23 g, 0.33 mmol) were dissolved in THF (30mL) and stirred at 75℃ for 4h under argon atmosphere. The solvent was removed under vacuum after the reaction mixture was cooled to ambient temperature. Compound 11 was purified by chromatography in a silica gel column eluting with hexanes/dichloromethane (2:1, v/v) as a brown-red oil. (3.79 g, 84% yield). ^{1}H NMR (400 MHz, Chloroform-*d*) δ 7.31 (d, *J* = 1.4 Hz, 2H), 7.22 (d, *J* = 1.2 Hz, 2H), 4.74 (d, *J* = 6.8 Hz, 2H), 2.53 (d, *J* = 7.0 Hz, 4H), 2.23 (p, *J* = 6.4 Hz, 1H), 1.75 – 1.62 (m, 10H), 1.52 (ddt, *J* = 14.8, 7.2, 3.7 Hz, 2H), 1.39 – 1.28 (m, 8H), 1.18 (ddd, *J* = 23.9, 13.6, 6.2 Hz, 6H), 0.99 – 0.86 (m, 10H).

Synthesis of 1,9-bis(cyclohexylmethyl)-5,10,11-tris(2-ethylhexyl)-10,11-dihydro-5*H*-thieno[2',3':4,5]pyrrolo[3,2-*g*]thieno[3,2-*b*][1,2,3]triazolo[4,5-*e*]indole (12)

Under argon, compound 11 (2.31 g, 3.41 mmol) and triphenylphosphine (8.93 g, 34.1 mmol) were dissolved in N-Methylpyrrolidone (NMP, 10 mL). The mixture was stirred at 180℃ overnight. After cooled to ambient temperature, to the mixture was added potassium hydroxide (1.91 g, 34.1 mmol), potassium iodide (136 mg, 0.82 mmol) and 1-bromo-2-ethylhexane (6.59 g, 34.1 mmol). The mixture was stirred at 90℃ overnight under argon atmosphere. The organic layer was washed with water and brine and dried with $MgSO_4$. Compound 12 was obtained by column chromatography in a silica gel column eluting with hexanes/dichloromethane (4:1, v/v) as a tawny oil (1.49 g, 52% yield). ^{1}H NMR (400 MHz, Chloroform-*d*) δ 6.95 (s, 2H), 4.70 (d, *J* = 7.2 Hz, 2H), 4.44 (s, 4H), 2.77 (d, *J* = 14.8 Hz, 4H), 2.42 – 2.29 (m, 1H), 1.74 (dd, *J* = 29.3, 15.2 Hz, 16H), 1.46 – 0.21 (m, 50H).

Synthesis of 1,9-bis(cyclohexylmethyl)-5,10,11-tris(2-ethylhexyl)-10,11-dihydro-5*H*-thieno[2',3':4,5]pyrrolo[3,2-*g*]thieno[3,2-*b*][1,2,3]triazolo[4,5-*e*]indole-2,8-dicarbaldehyde (13)

Under argon, LDA (2 mol L^{-1}, 11.9 mmol) was added dropwise into a solution of compound 12 (01 g, 1.19 mmol) in dry THF (20 mL) at -78℃. The mixture was then stirred for 1h. Dry DMF (5 mL) was added, after string at -78℃ for another 30 min, the mixture was warmed to room temperature and reacted overnight. The mixture was poured into water (200 mL) and extracted with DCM. The organic layer was washed with water, dried by $MgSO_4$. Removing the solvent and the crude product was purified by column chromatography in a silica gel column, eluting with petroleum ether/dichloromethane (1:1, v/v) to give compound 13 as an orange solid. (0.91 g, 86% yield). ^{1}H NMR (400 MHz, Chloroform-*d*) δ 10.11 (s, 2H), 4.71 (d, *J* = 6.9 Hz, 2H), 4.47 (d, *J* = 7.2 Hz, 4H), 3.48 – 3.31 (m, 2H), 3.04 – 2.86 (m, 2H), 2.36 – 2.27 (m, 1H), 1.91 – 1.59 (m, 16H), 1.46 – 1.05 (m, 28H), 0.99 – 0.18 (m, 22H).

Synthesis of 2,2'-((2Z,2'Z)-((1,9-bis(cyclohexylmethyl)-5,10,11-tris(2-ethylhexyl)-10,11-dihydro-5*H*-thieno[2',3':4,5]pyrrolo[3,2-*g*]thieno[3,2-*b*][1,2,3]triazolo[4,5-*e*]indole-2,8-diyl)bis(methaneylylidene))bis(5,6-difluoro-3-oxo-2,3-dihydro-1*H*-indene-2,1-diylidene))dimalononitrile (BZ4F-ch2)

Under argon, compound 13 (0.247 g, 0.276 mmol) and 2-(5,6-difluoro-3-oxo-2,3-dihydro-1H-inden-1-ylidene)malononitrile (153 mg, 0.66 mmol) were dissolved in toluene (10 mL). To the mixture boron trifluoride etherate ($BF_3{\cdot}OEt_2$, 0.5 mL) and acetic anhydride (0.5 mL) were added. After stirring at room temperature for 0.5 h, the mixture was poured into methanol and filtered. The residue was purified in a silica gel column using petroleum ether/dichloromethane (1:2, v/v) as the eluent. BZ4F-ch2 was obtained as a black-red solid powder (332 mg, 91% yield). ^{1}H NMR (400 MHz, Chloroform-*d*) δ 9.22 (s, 2H), 8.58 (dd, *J* = 9.9, 6.5 Hz, 2H), 7.73 (t, *J* = 7.4 Hz, 2H), 4.73 (d, *J* = 6.3 Hz, 2H), 4.63 – 4.35 (m, 4H), 3.48 (dd, *J* = 15.6, 5.6 Hz, 2H), 3.01 (dd, *J* = 12.9, 5.5 Hz, 2H), 2.43 (s, 1H), 1.89 – 1.63 (m, 14H), 1.32 (dddd, *J* = 41.0, 33.3, 18.8, 7.9 Hz, 26H), 1.06 – 0.06 (m, 26H). ^{13}C NMR (101 MHz, Chloroform-*d*) δ 185.88, 159.44, 153.14, 153.01, 146.78, 142.70, 138.40, 136.67, 136.60, 136.09, 135.97, 134.61, 120.40, 115.50, 115.03, 114.80, 112.62, 112.44, 112.09, 68.18, 60.21, 52.55, 41.45, 40.45, 40.34, 39.91, 35.09, 33.38, 33.18, 30.63, 30.16, 28.49, 28.25, 27.82, 26.55, 26.27, 26.19, 24.80, 24.13, 23.71, 22.96, 22.47, 21.46, 14.00, 13.80, 13.28, 11.11, 10.58, 7.58. MALDI-TOF MS: calcd for $C_{78}H_{83}F_4N_9O_2S_2$ (M^+), 1317.6047; found, 1317.5782。

4. Spectral Charts of NMR

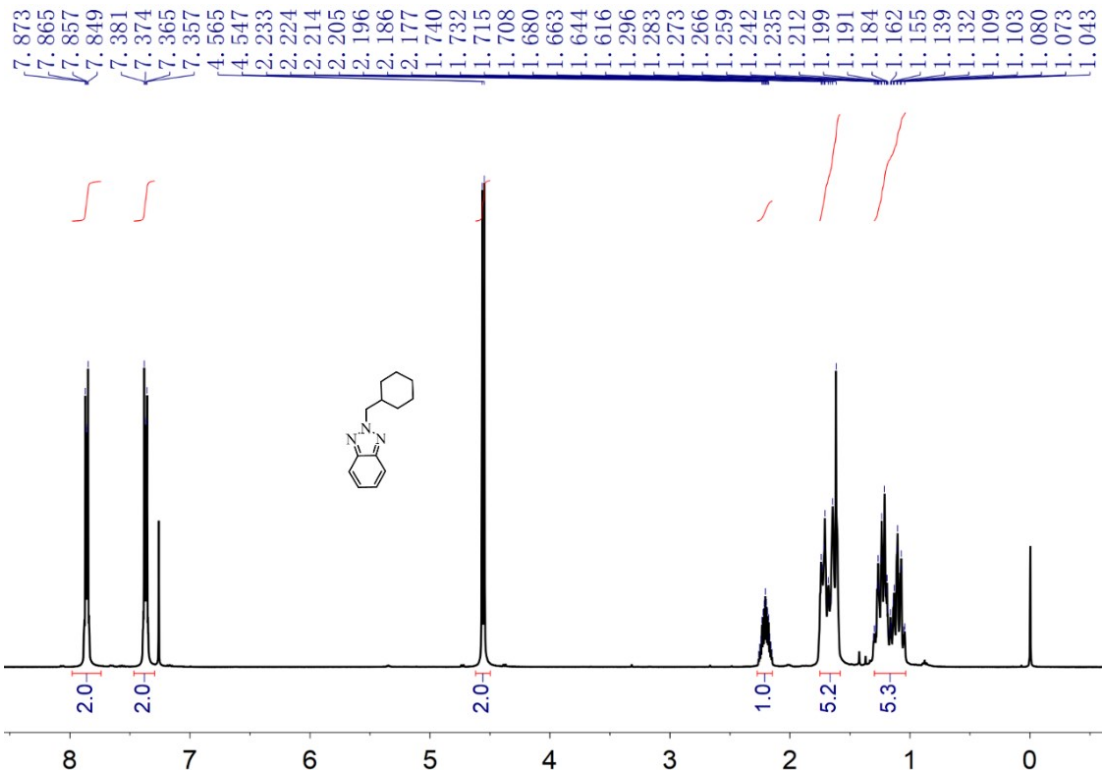

Fig. S1 ^{1}H NMR spectrum of compound 1 ($CDCl_3$).

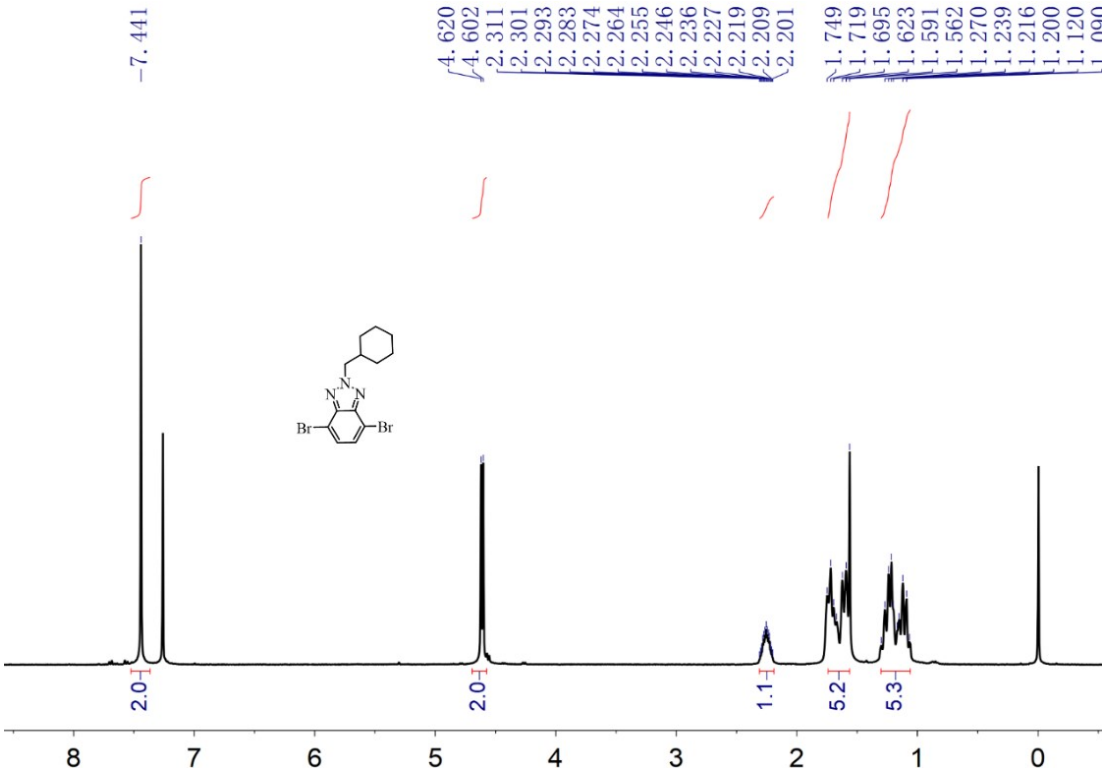

Fig. S2 ^{1}H NMR spectrum of compound 2 ($CDCl_3$).

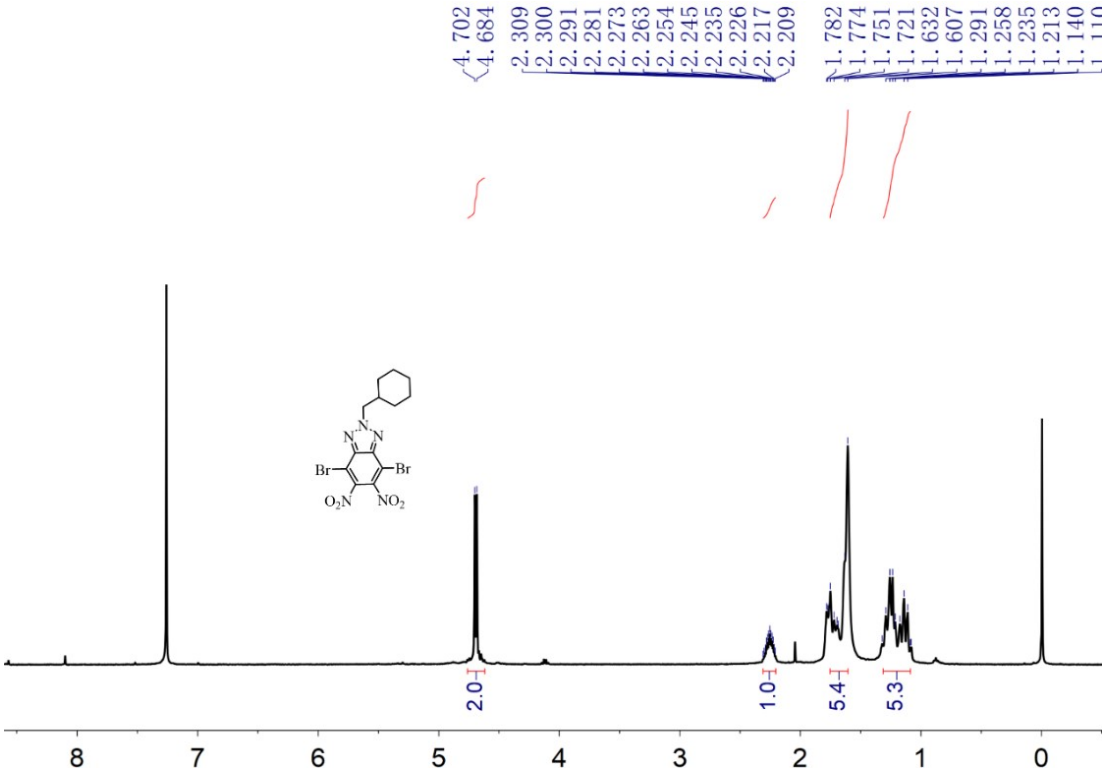

Fig. S3 ^{1}H NMR spectrum of compound 3 ($CDCl_3$).

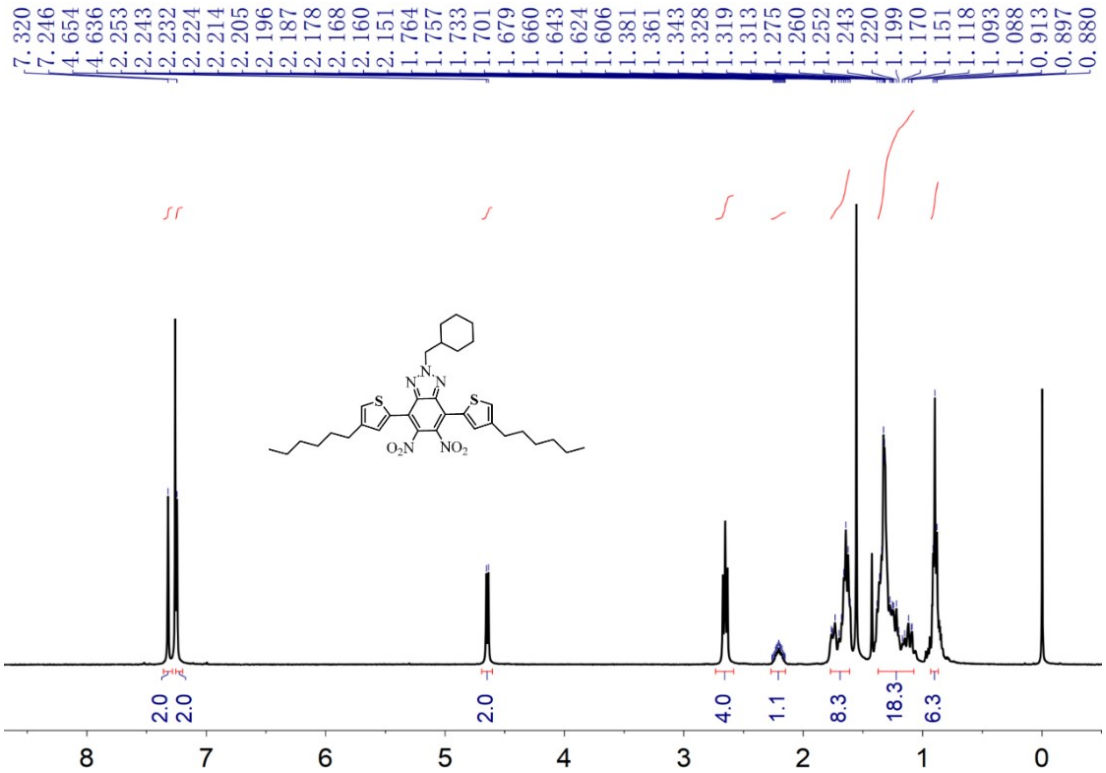

Fig. S4 ^{1}H NMR spectrum of compound 5 ($CDCl_3$).

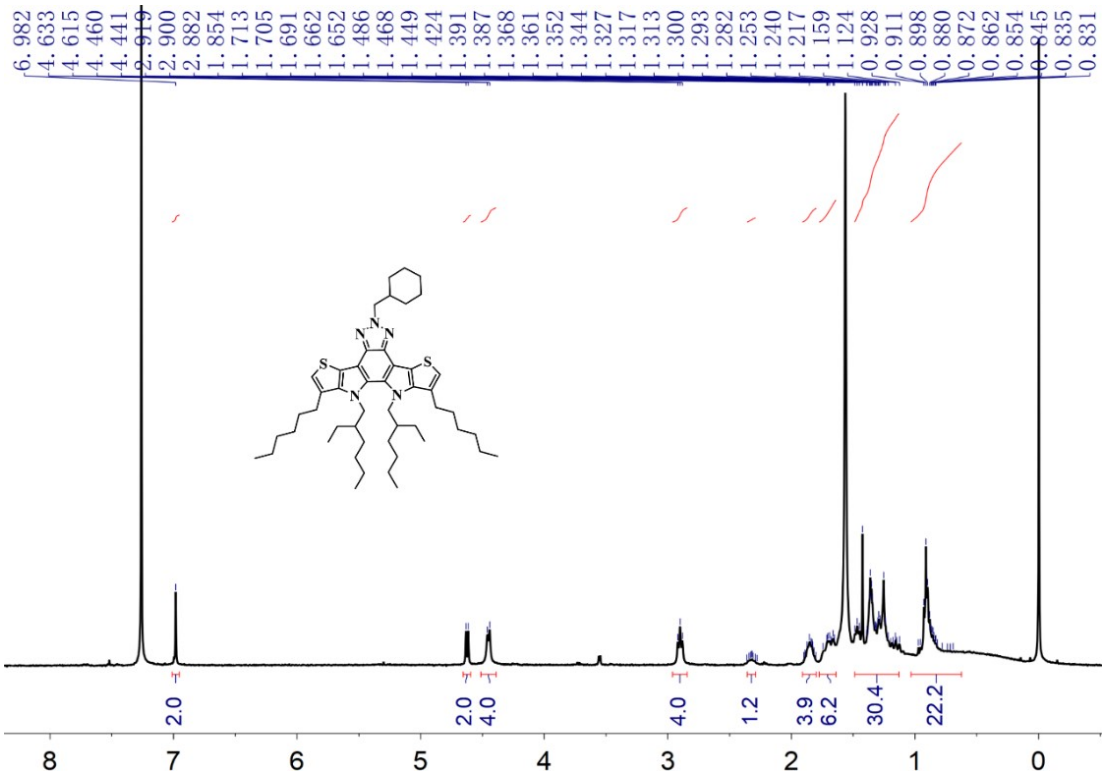

Fig. S5 ^{1}H NMR spectrum of compound 6 ($CDCl_3$).

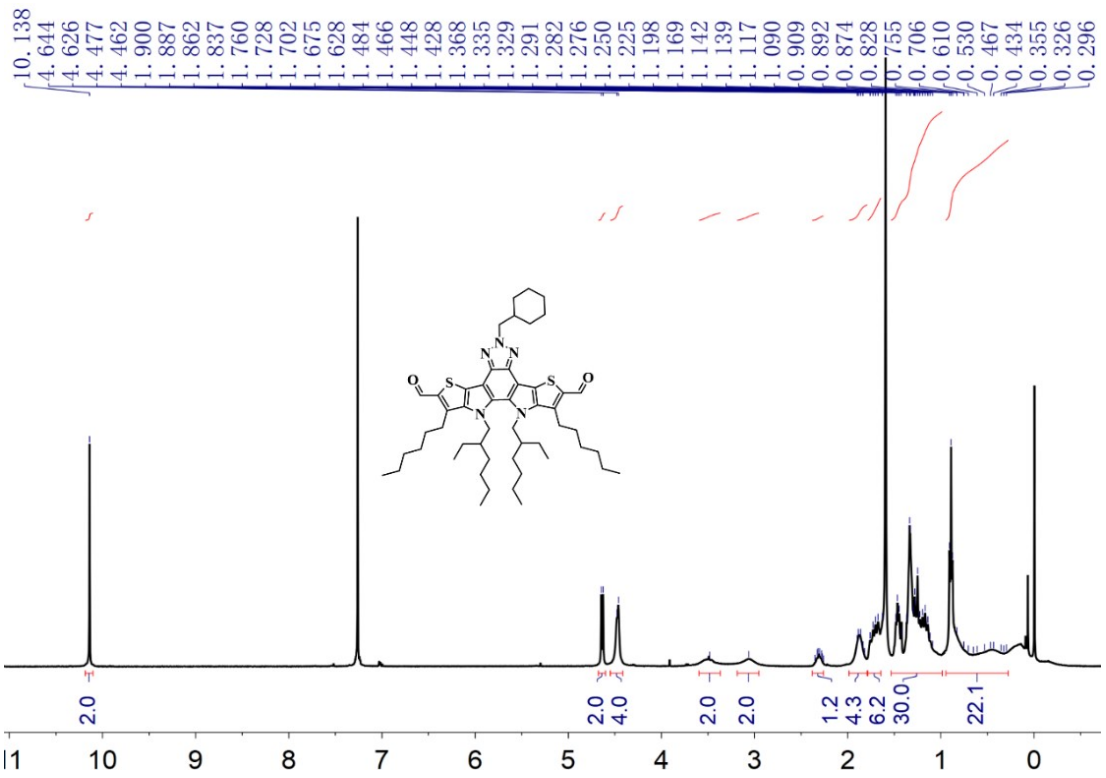

Fig. S6 ^{1}H NMR spectrum of compound 7 ($CDCl_3$).

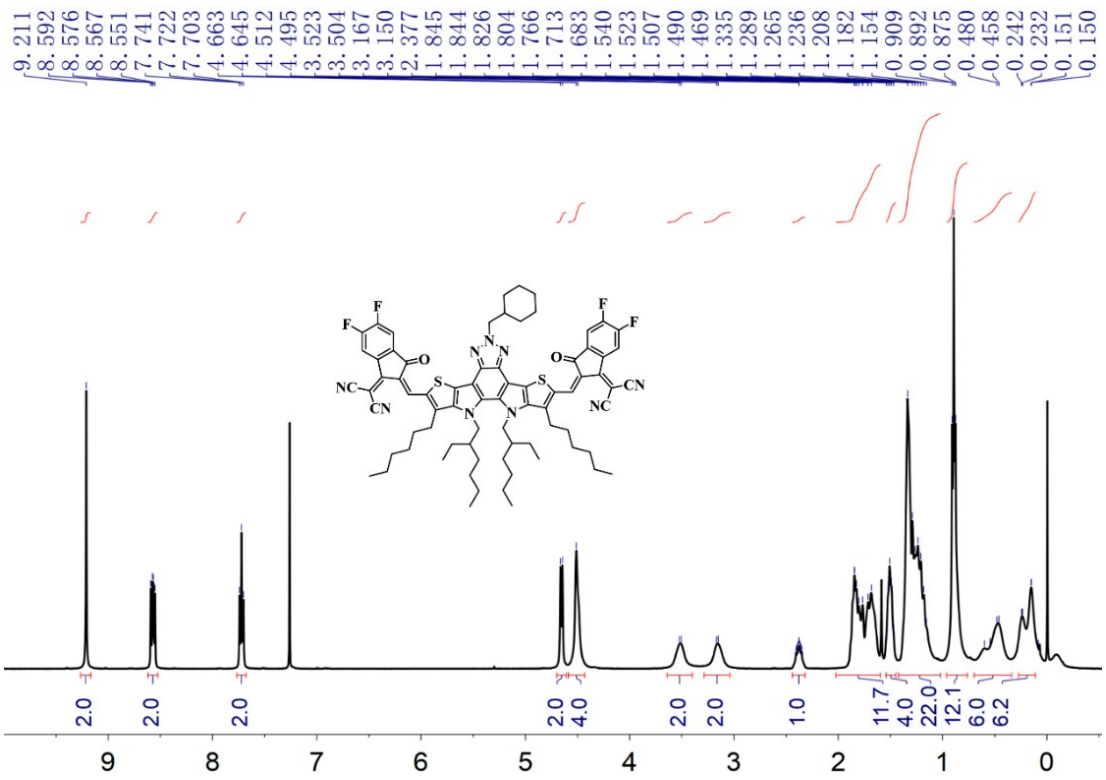

Fig. S7 ^{1}H NMR spectrum of BZ4F-ch1 ($CDCl_3$).

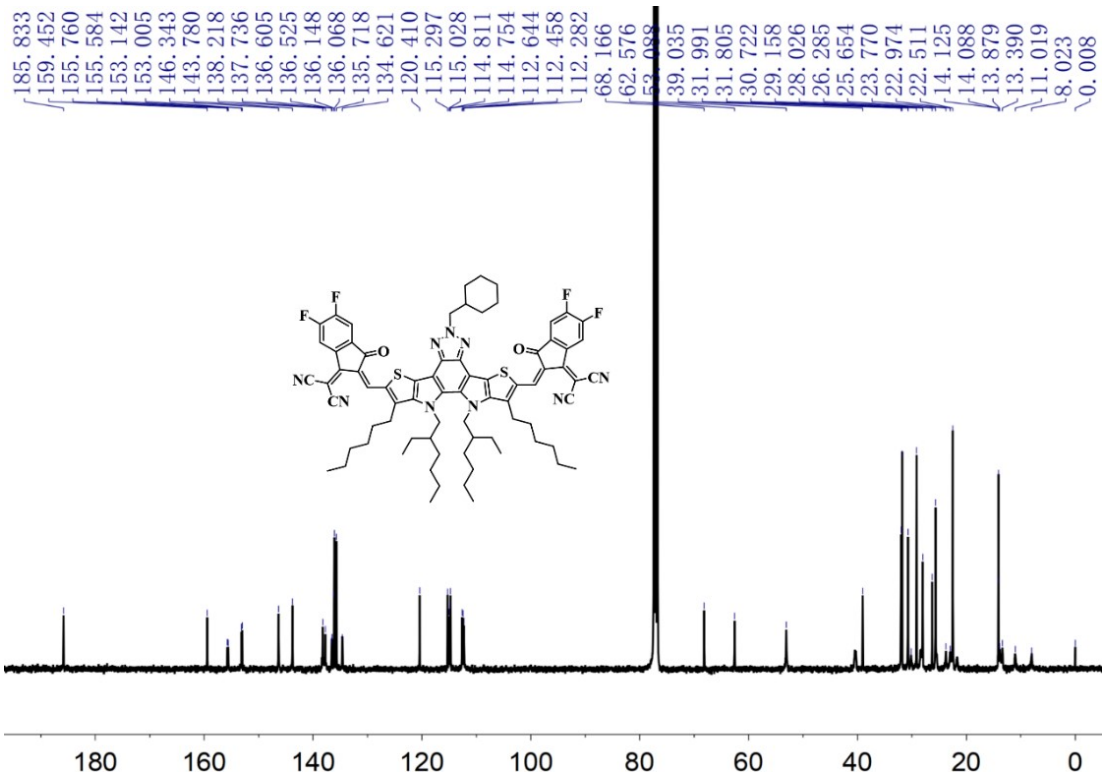

Fig. S8 ^{13}C NMR spectrum of BZ4F-ch1 ($CDCl_3$).

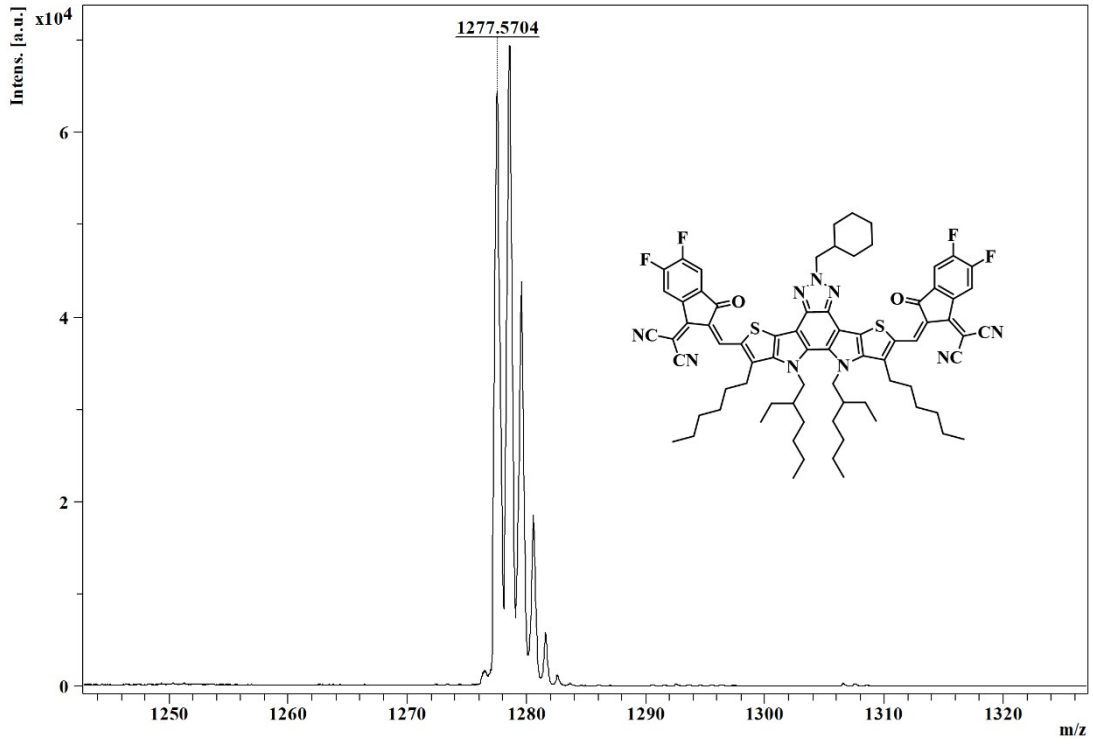

Fig. S9 The mass spectrum (MALDI-TOF) of BZ4F-ch1.

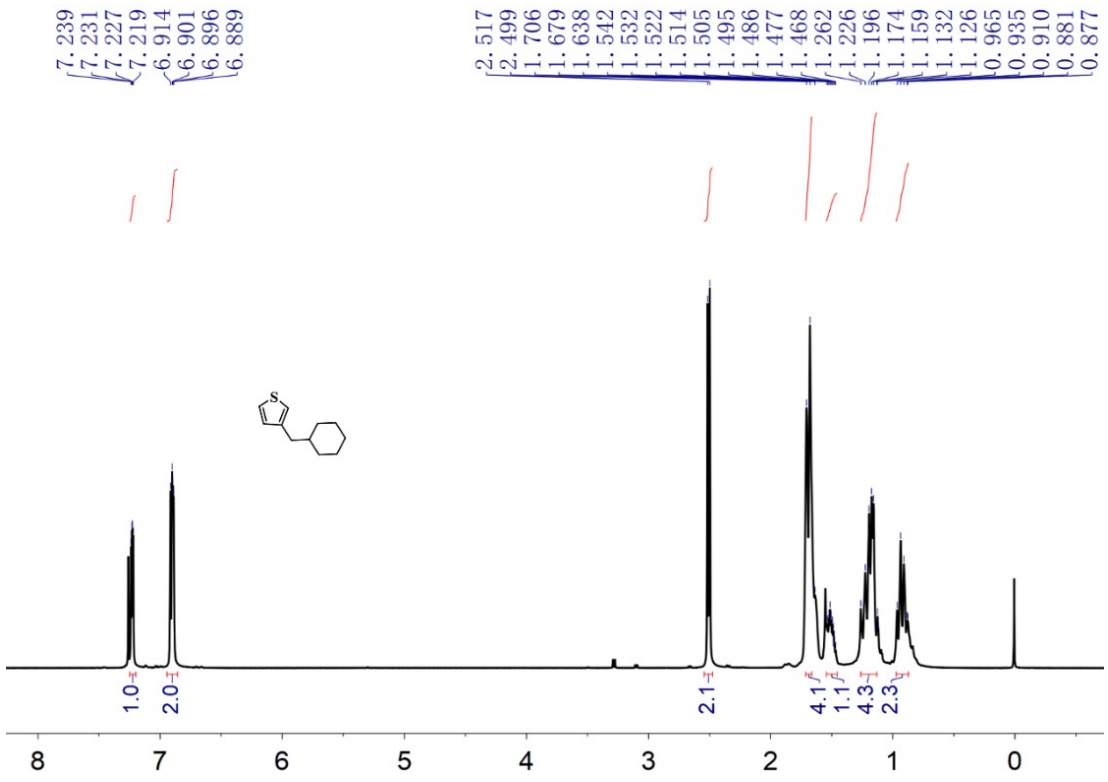

Fig. S10 ^{1}H NMR spectrum of compound 8 ($CDCl_3$).

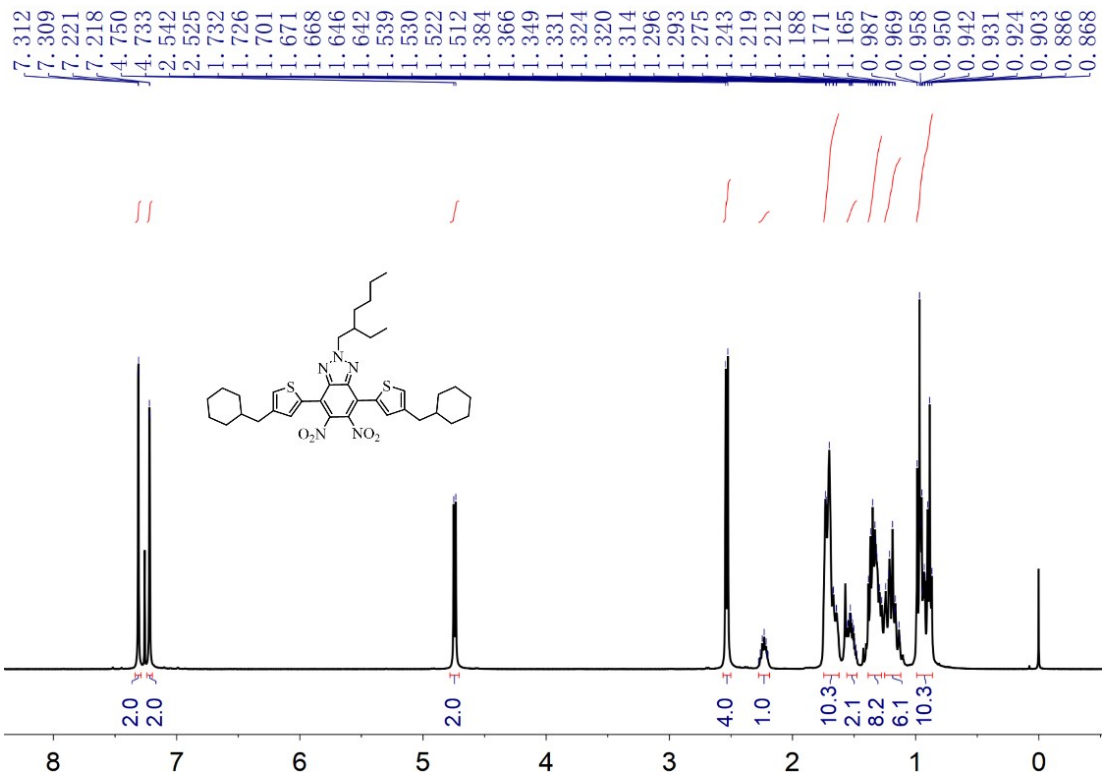

Fig. S11 ^{1}H NMR spectrum of compound 11 ($CDCl_3$).

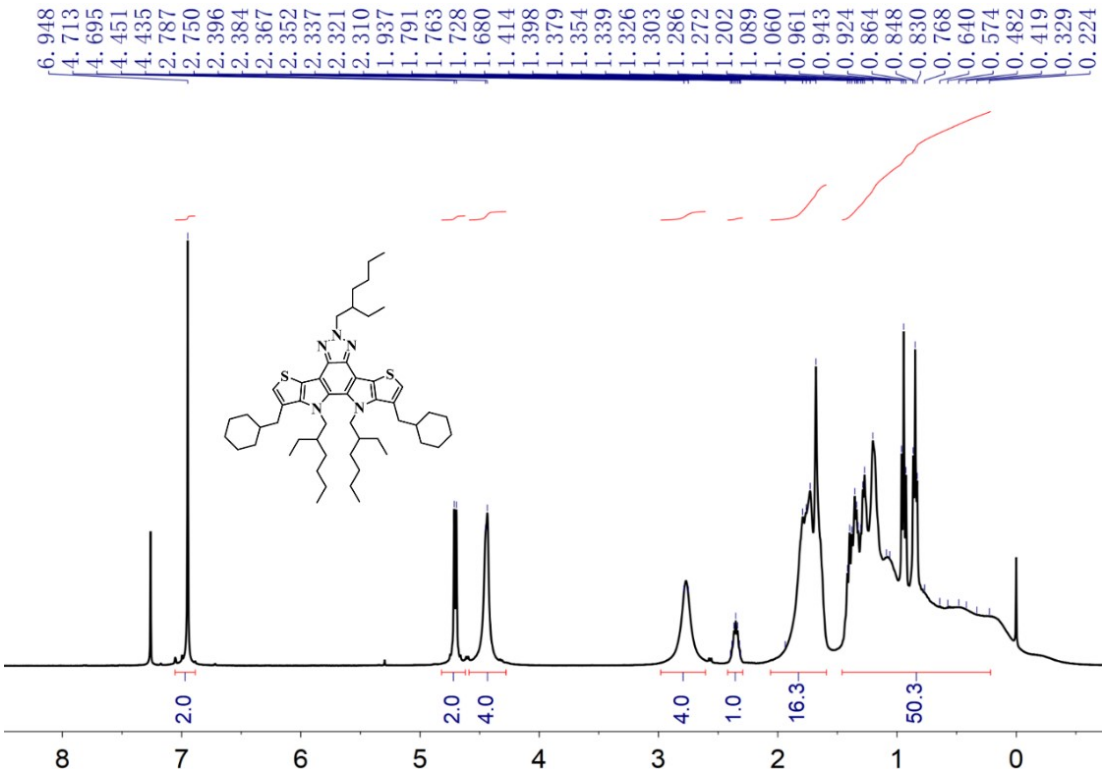

Fig. S12 ^{1}H NMR spectrum of compound 12 ($CDCl_3$).

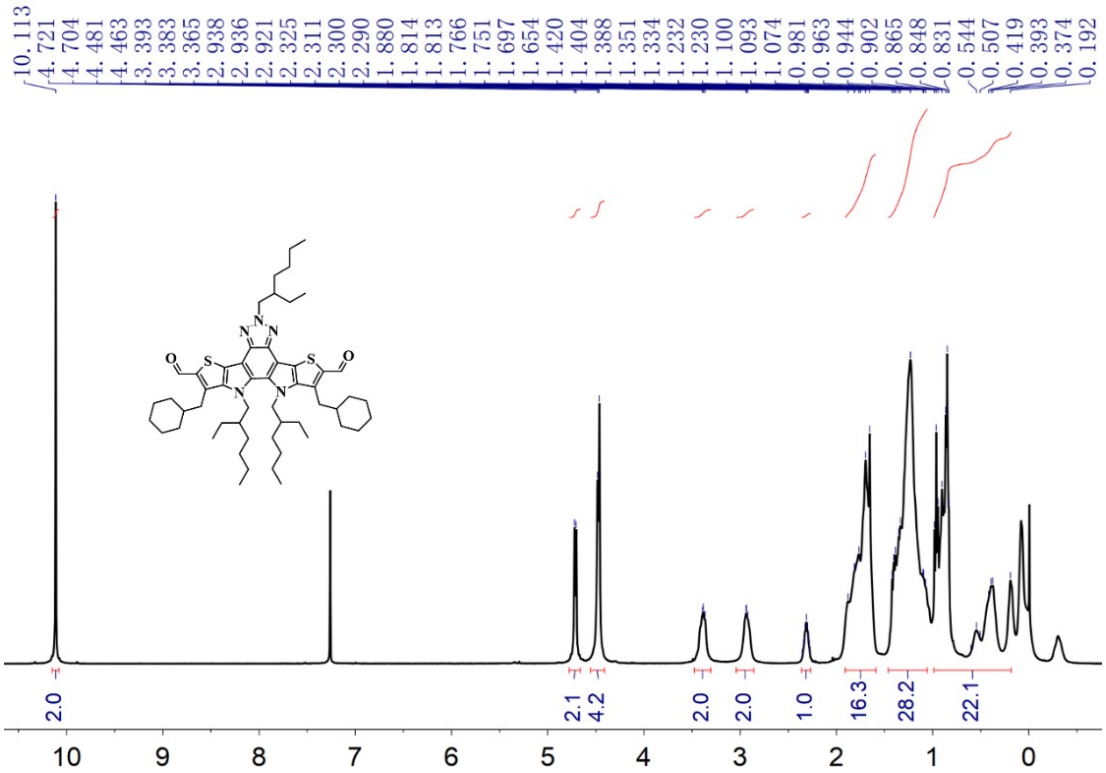

Fig. S13 ^{1}H NMR spectrum of compound 13 ($CDCl_3$).

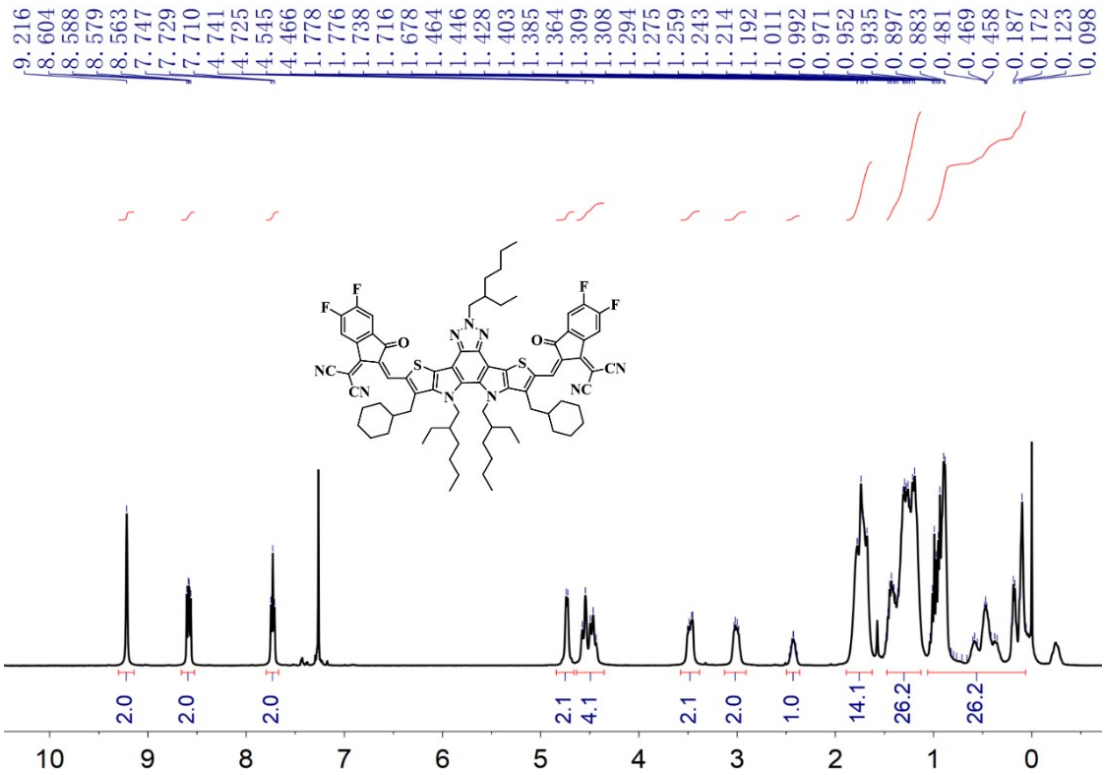

Fig. S14 ^{1}H NMR spectrum of BZ4F-ch2 ($CDCl_3$).

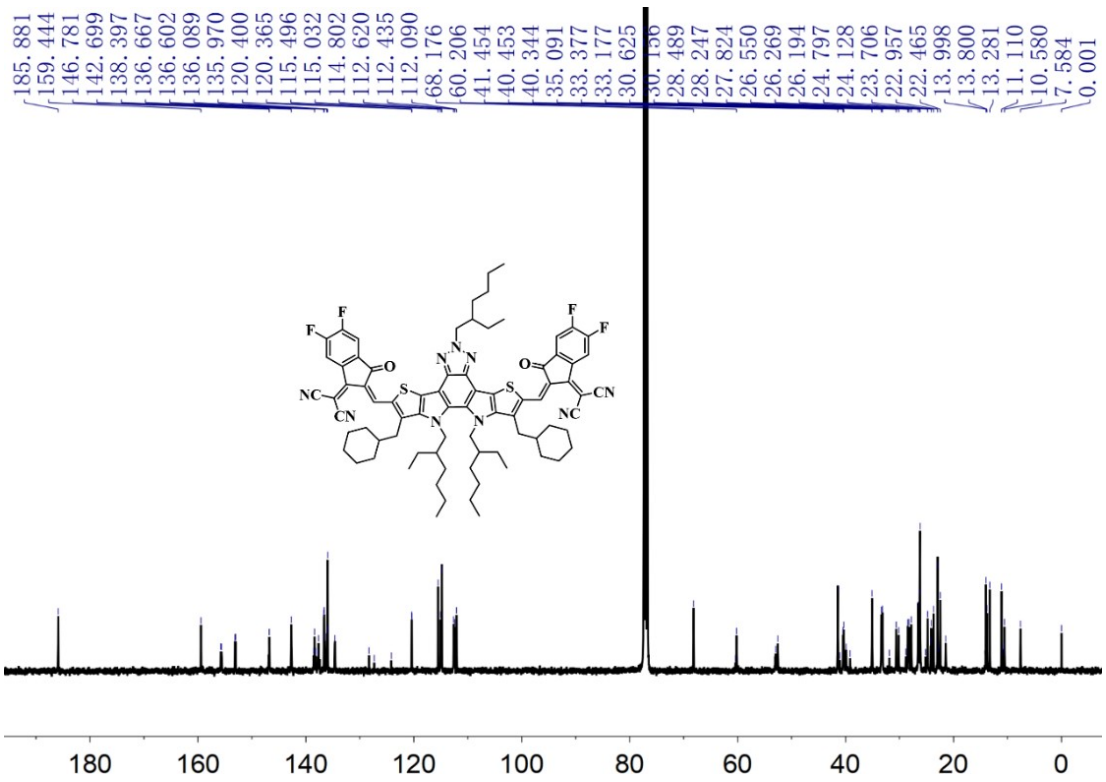

Fig. S15 ^{13}C NMR spectrum of BZ4F-ch2 ($CDCl_3$).

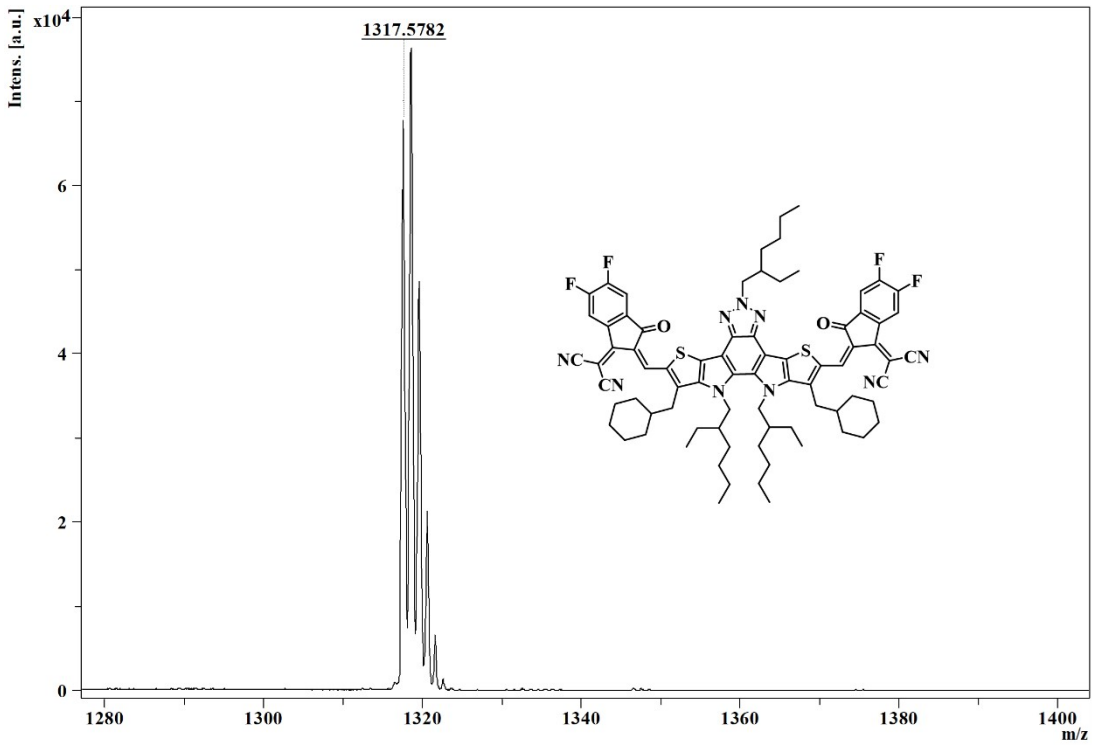

Fig. S16 The mass spectrum (MALDI-TOF) of BZ4F-ch2.

4. Additional Figures

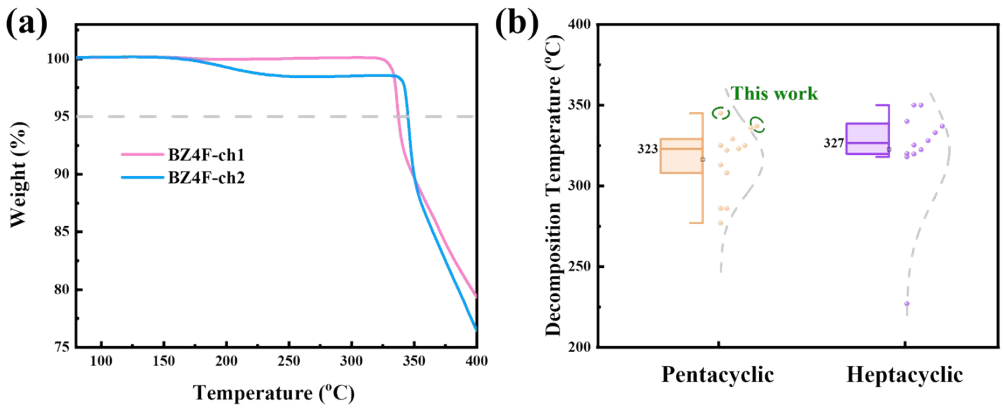

Fig. S17 (a) Thermogravimetric analysis curves of BZ4F-ch1 and BZ4F-ch2 with a heating rate of 10 °C·min^{-1}; (b) the decomposition temperature (T_d, 5% weight loss) of A-DA′D-A type pentacyclic and heptacyclic small molecule acceptors.

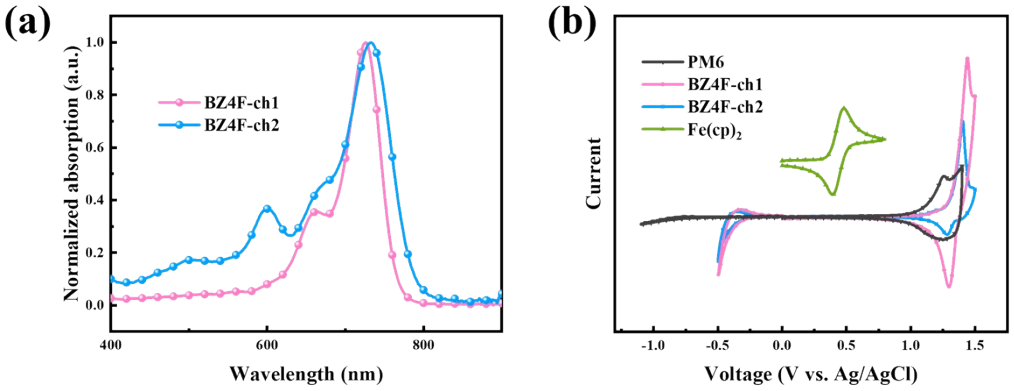

Fig. S18 (a) The normalized absorption spectra of BZ4F-ch1 and BZ4F-ch2 in CF; (b) the CV curves of PM6, BZ4F-ch1 and BZ4F-ch2 in solid state.

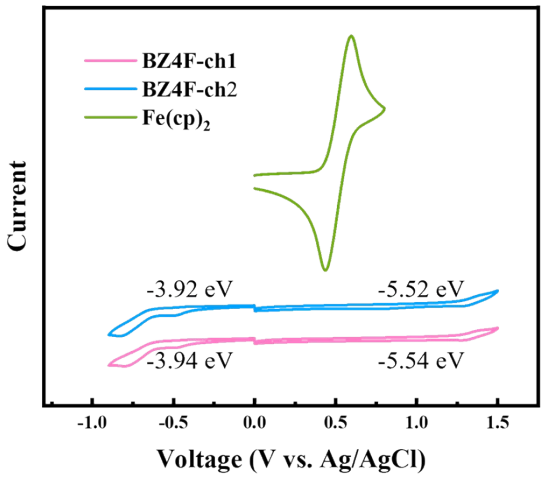

Fig. S19 The CV curves of BZ4F-ch1 and BZ4F-ch2 in solution state.

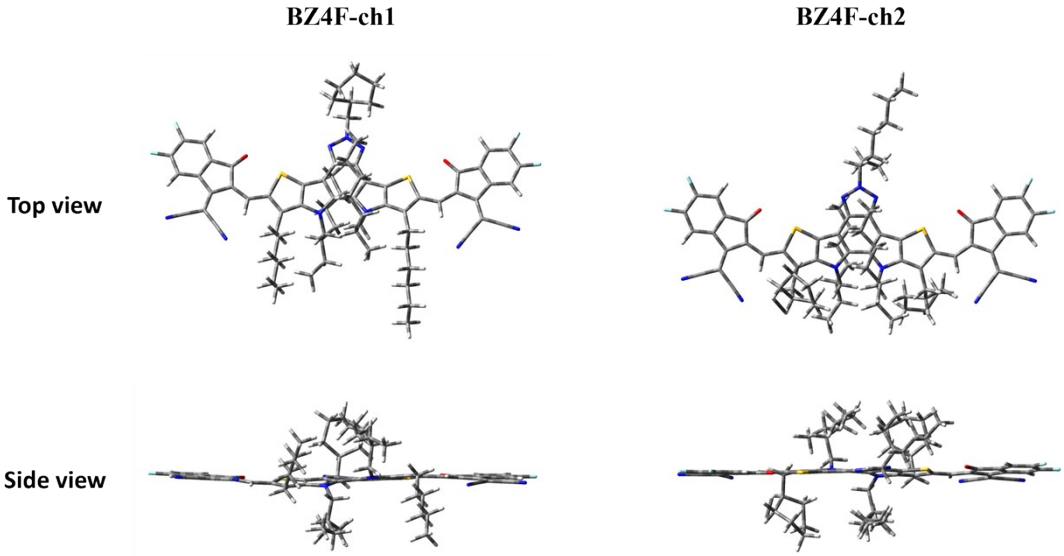

Fig. S20 The optimized geometries (top and side view) of BZ4F-ch1 and BZ4F-ch2.

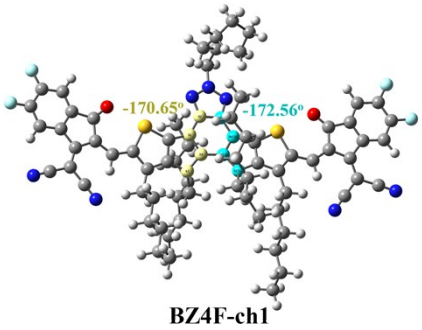

BZ4F-ch1

Dihedral angle	BZ4F-ch1	BZ4F-ch2
N-C-C-C (left)	-170.65°	-170.93°
N-C-C-C (right)	-172.56°	-174.2°
left - right	1.91°	3.27°

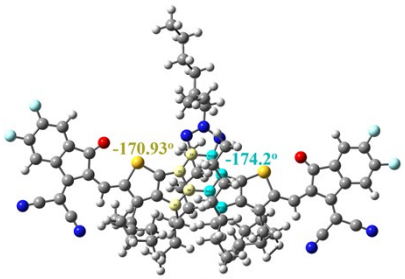

BZ4F-ch2

Fig. S21 The dihedral angle of two N-C-C-C in the optimized BZ4F-ch1 and BZ4F-ch2, the "left-right" angle is used to evaluate the planarity of the two pyrrole moieties.

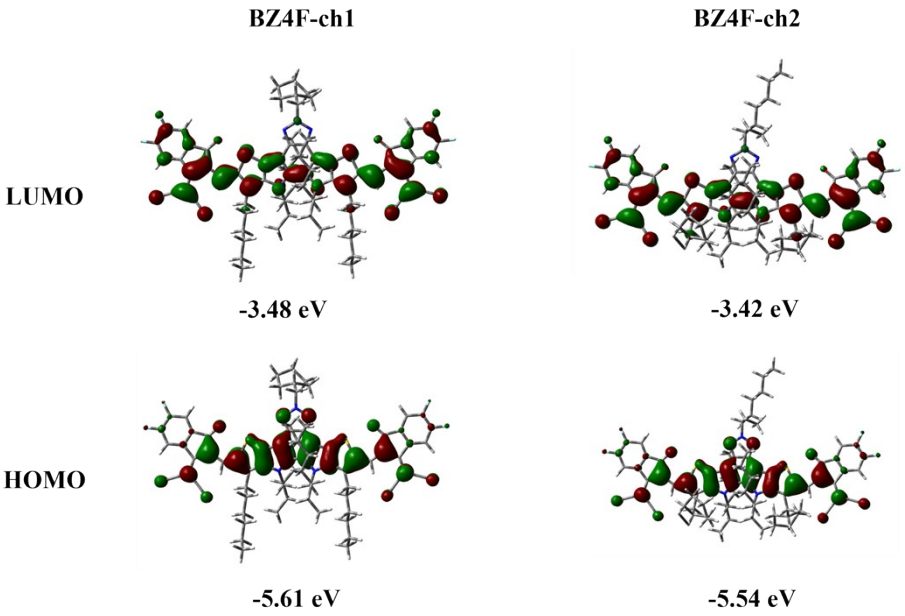

Fig. S22 The HOMO and LUMO energy levels of BZ4F-ch1 and BZ4F-ch2 calculated by DFT.

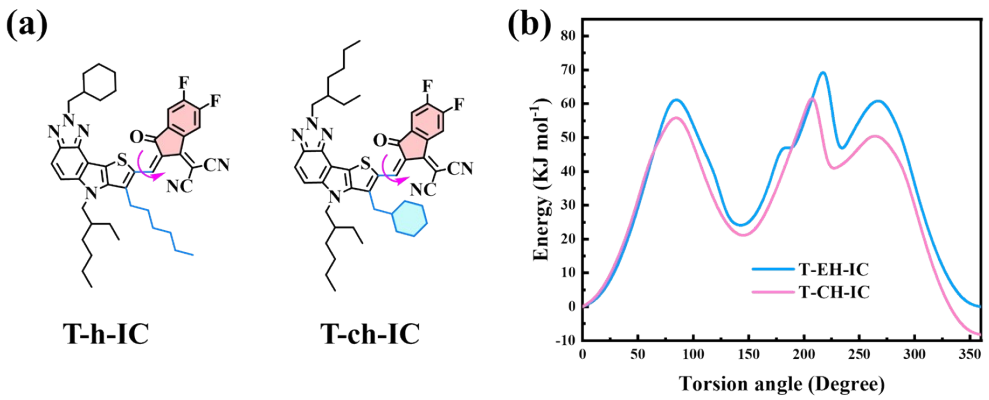

Fig. S23 (a) Sketch of torsion for T-h-IC and T-ch-IC; (b) relaxed potential energy scan curves for T-h-IC and T-ch-IC.

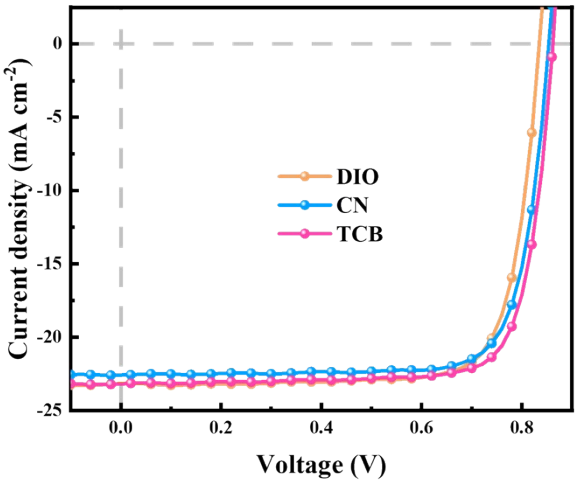

Fig. S24 *J-V* curves of the PM6: BZ4F-ch1 based devices with different additives.

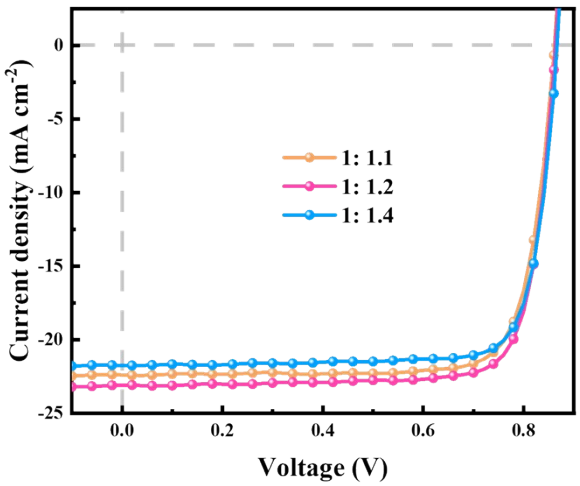

Fig. S25 *J-V* curves of the PM6: BZ4F-ch1 based devices with different D:A weight ratio.

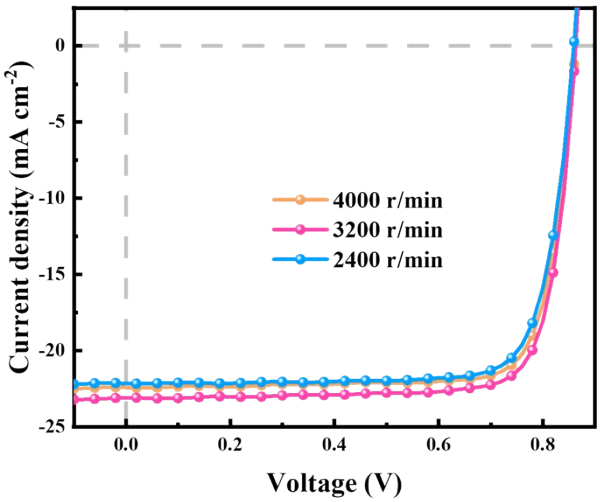

Fig. S26 *J-V* curves of the PM6: BZ4F-ch1 based devices with different spin-coating speed of the active layer.

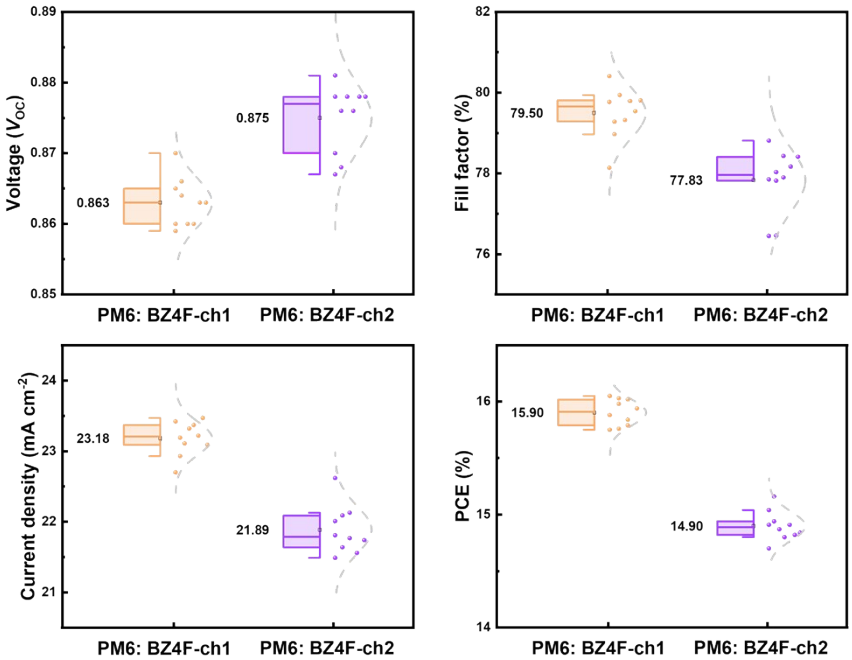

Fig. S27 The data statistics of photovoltaic parameters of the PM6: BZ4F-ch1 and PM6: BZ4F-ch2 based devices from 10 individual devices.

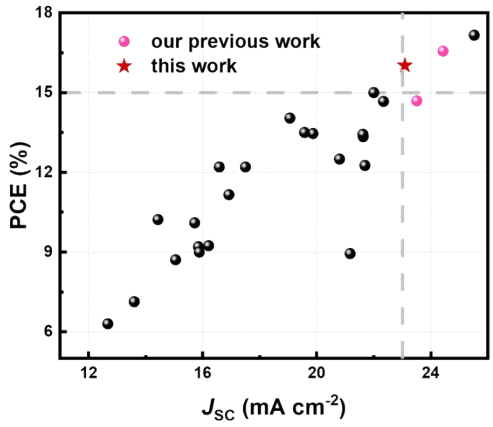

Fig. S28 Statistics of PCE – J_{SC} scatters for binary OSCs based on pentacyclic fused-ring acceptors.

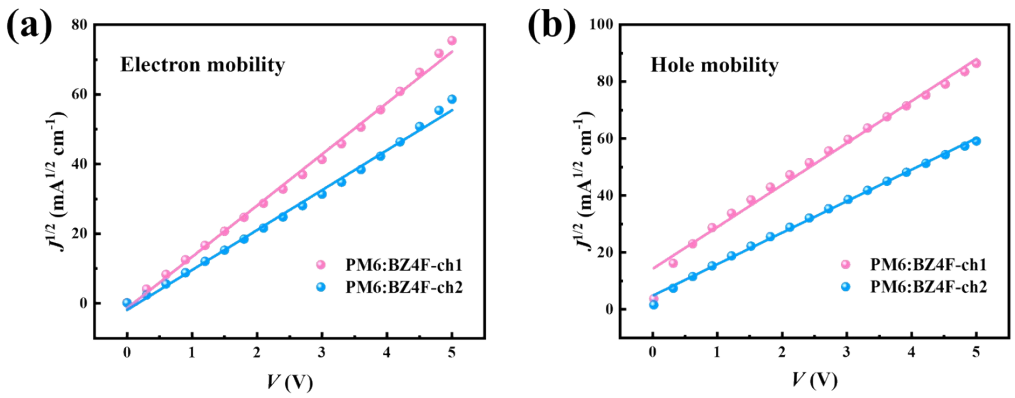

Fig. S29 (a) Electron mobility and (b) hole mobility of the optimized OSCs based on PM6: BZ4F-ch1 and PM6: BZ4F-ch2.

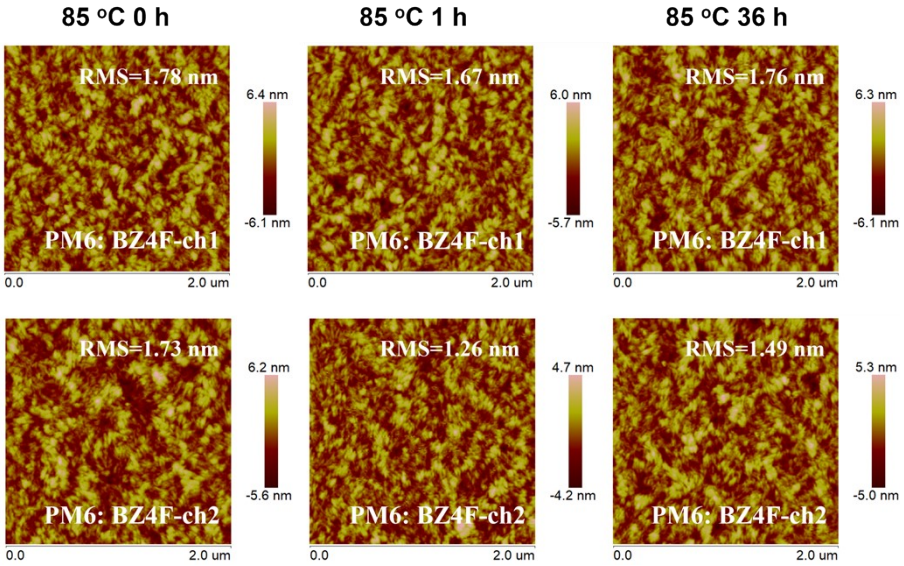

Fig. S30 AFM images of the active blends under thermal stress at 85 °C for 0, 1 and 36 hours, respectively.

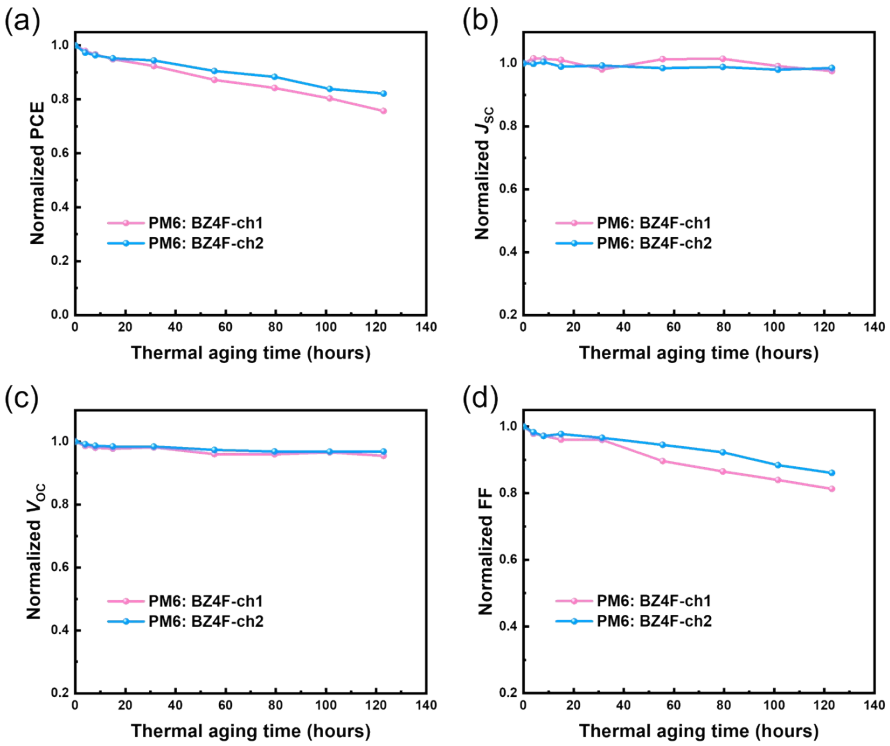

Fig. S31 Thermal stability of the unencapsulated PM6: BZ4F-ch1 and PM6: BZ4F-ch2 based OSCs in a N_2 glovebox.

5. Additional Tables and Schemes

Table S1. The thermal decomposition temperature (T_d, 5% weight loss) of SMAs.

Acceptors	T_d (°C)	Ref.
BZIC	325	2
Y25	322	1
Y26	313	1
BZ4F-O-1	308	3
BZ4F-O-2	286	3
BZ4F-O-3	277	3
BZ4F-EH	329	4
BZ4F-OEH	286	4
BTPT4F-EH	323	5
BTPT4F-BO	325	5
BTPT4F-HD	336	5

BZ4F-ch1	337	This work
BZ4F-ch2	345	This work
Y5	340	[6]
Y6	318	[7]
Y1	350	[8]
Y2	350	[8]
L8-BO	320	[9]
BTIC-4EO-4F	325.3	[10]
BTIC-4EO-4Cl	322.4	[10]
BTIC-4EO-4Br	319.7	[10]
Y6-1O	328	[11]
Y6-2O	333	[11]
Y6-Se	227	[12]
Y6-2Se	337	[12]

Table S2. The photovoltaic parameters of the PM6: BZ4F-ch1 based devices with different additives.

Additives	V_{OC} (V)	J_{SC} (mA cm^{-2})	FF (%)	PCE (%)
DIO	0.835	23.16	78.68	15.09
CN (0.5v%)	0.854	22.58	78.71	15.06
TCB (10 mg/mL)	0.862	23.19	79.14	15.70

All the devices are optimized by regulating the spin-coating speed of active layer.

Table S3. The photovoltaic parameters of the PM6: BZ4F-ch1 based devices with different D: A weight ratio.

D: A weight ratio	V_{OC} (V)	J_{SC} (mA cm^{-2})	FF (%)	PCE (%)
1:1	0.861	22.40	80.04	15.44
1:1.2	0.863	23.09	80.41	16.02
1:1.4	0.866	21.76	80.92	15.25

All the devices are fabricated with the TCB additive.

Table S4. The photovoltaic parameters of the PM6: BZ4F-ch1 based devices with different spin-coating speed of the active layer.

Speed	V_{OC} (V)	J_{SC} (mA cm^{-2})	FF (%)	PCE (%)
4000	0.862	22.42	80.20	15.51
3200	0.863	23.09	80.41	16.02
2400	0.859	22.15	79.60	15.15

All the devices are fabricated with the D: A weight ratio of 1:1.2.

Table S5. The device parameters of the binary OSCs based on pentacyclic SMAs.

Donor: Acceptor	V_{OC} (V)	J_{SC} (mA cm^{-2})	FF (%)	PCE (%)	E_g^{opt} (eV)	Ref.
PDBT-T1: IC-C6IDT-IC	0.89	15.05	63	8.71	1.62	[13]
PDBT-T1: IC-C6IDT-IC	0.85	15.85	65	9.2	1.62	[14]
HFQx-T: BZIC	0.84	12.67	59	6.3	1.45	[2]
PBDB-T: IDT-N	0.79	15.88	71.91	9	1.58	[15]
PM6: IDTN	0.946	16.58	78	12.2	1.59	[16]
PBDB-T: NBDTP	0.937	15.72	66.4	10.1	1.58	[17]
PBDB-T: IDT-HN	0.93	14.43	76.41	10.22	1.68	[18]
FTAZ: IDIC	0.84	20.8	71.8	12.5	1.60	[19]
PTQ10: IDTPC	0.93	17.5	74.6	12.2	1.52	[20]
PBDB-T2Cl: IDIC-4Cl	0.83	16.21	68.69	9.24	1.58	[21]
FTAZ: IDIC1	0.896	13.6	58.5	7.13	1.67	[22]
BSFTR: NBDTP-F_{out}	0.797	21.69	70.93	12.26	1.41	[23]
PM6: DTP-C_{17}-4F	0.691	21.17	61.1	8.94	1.38	[24]
PTQ10: MO-IDIC	0.969	16.92	68.1	11.16	1.60	[25]
PTQ10: MO-IDIC-2F	0.906	19.87	74.8	13.46	1.55	[25]
PM6: IDIC-C4Ph	0.941	19.06	78.32	14.04	1.62	[26]
PM6: Y26	0.83	21.63	74.33	13.34	1.46	[1]
PM6: BZ4F-O-3	0.847	23.51	73.72	14.69	1.40	[3]
PM6: BZ4F-OEH	0.855	24.43	79.3	1.40	16.56	[4]
PM6: BZ4F-EH	0.880	22.34	75.1	1.47	14.67	[4]
PM6: BTA-C4-Cl	0.894	25.52	75.26	1.44	17.16	[27]

PM6: BZ4F-ch1	0.863	23.09	80.41	1.44	16.02	This work
PM6: BZ4F-ch2	0.878	22.01	77.85	1.45	15.04	This work

Table S6. GIWAXS data of the PM6, BZ4F-ch1, BZ4F-ch2 neat films and PM6: BZ4F-ch1 and PM6: BZ4F-ch2 blend films

Films	Out of plane			
	Location ($Å^{-1}$)	*d*-spacing[a] (Å)	FWHM ($Å^{-1}$)	CCL[b] (Å)
PM6	1.67	3.76	0.232	24.37
BZ4F-ch1	1.755	3.58	0.277	20.41
BZ4F-ch2	1.761	3.57	0.285	19.84
PM6: BZ4F-ch1	1.764	3.56	0.216	26.18
PM6: BZ4F-ch2	1.19	3.66	0.253	22.35

[a] Obtained using the equation of $d = 2\pi/q$, in which q is the corresponding *x*-coordinate of the diffraction peak. [b] Calculated using the equation: $CCL = 2\pi K/w$, in which w is the full-width-at-half-maximum and *K* is a form factor (0.9 here).

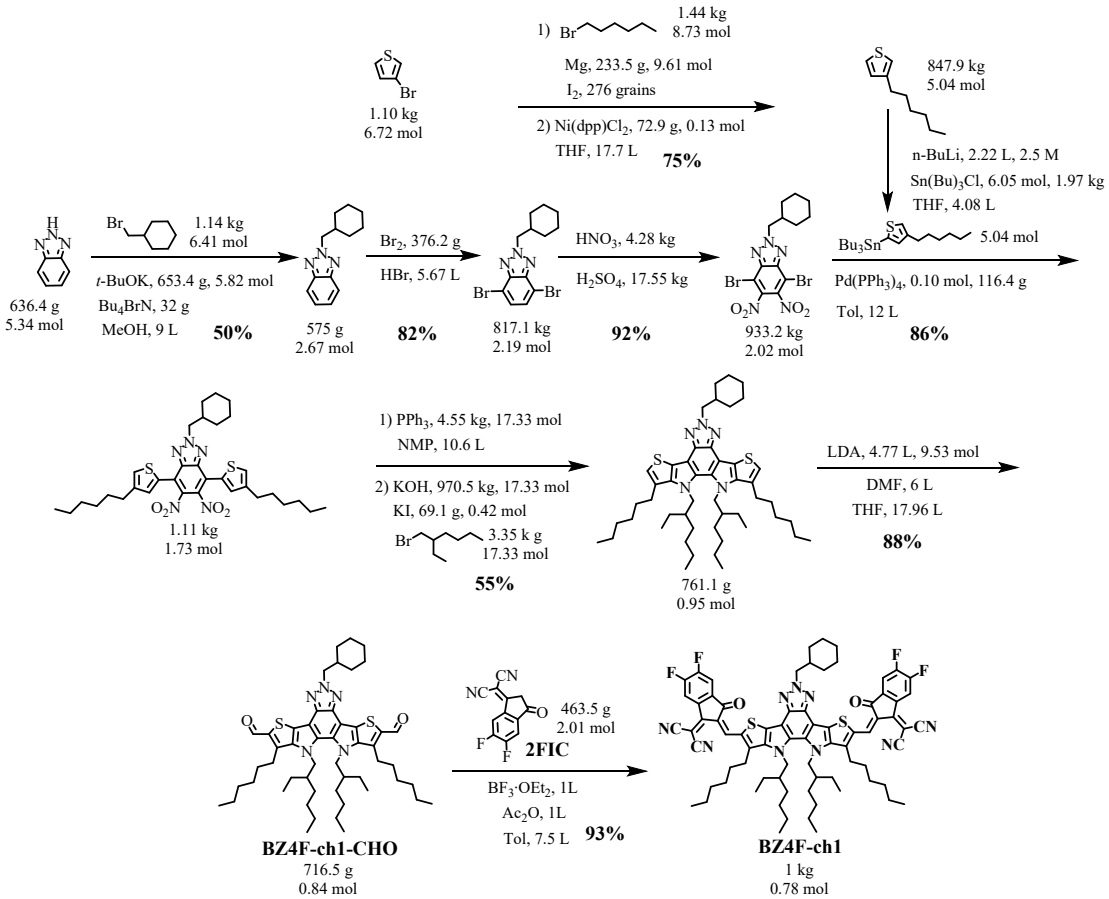

Scheme S3. The detailed synthetic route and the yield of each step of BZ4F-ch1.

Table S7. The MOC (material only cost) evaluation of BZ4F-ch1.

BZ4F-ch1-CHO (742.3 g)			
Reagent	Quantity	Unit price	Cost (CNY/dollar)
toluene	19.5 L	315CNY/10 L, Greagent	614.3/84.8
BF_3 OEt_3	1 L	680.11CNY/2.5 L, Aladdin	272/37.5
AC_2O	1 L	60CNY/500 mL, Greagent	120/16.6
LDA	4.77 L	230CNY/1 L, Energy Chemical	1097.1/151.4
THF	39.74 L	1200CNY/16 L, Energy Chemical	2980.5/411.4
DMF	6 L	950CNY/25 L, Energy Chemical	228/31.5
NMP	10.6 L	1795CNY/16 L, Adamas	1189.2/164.1
PPh_3	4.55 kg	2589CNY/25 kg, Energy Chemical	471.2/65
KOH	970.5 g	28CNY/500 g, Energy Chemical	54.3/7.5
KI	69.1 g	65CNY/100 g, Adamas	45/6.2
1-bromo-2-ethylhexane	3.35 kg	304CNY/2.5 kg, Adamas	407.4/56.2
n-BuLi	2.22 L	290CNY/1 L, Energy Chemical	643.8/88.9
$Sn(Bu)_3Cl$	1.97 kg	946.33CNY/2.5 kg, Adamas	745.7/102.9
$Pd(PPh_3)_4$	116.4 g	3495CNY/100 g, Adamas	4068.2/561.5
HNO_3	4.28 kg	500CNY/25 kg, Greagent	85.6/11.8

H_2SO_4	17.55 kg	350CNY/25 kg, Greagent	245.7/33.9
HBr	5.67 L	169.4CNY/2.5 L, Adamas	384.2/53
Br_2	376.2 g	220CNY/500 g, Chron Chemicals	165.5/22.8
2H-benzo[d][1,2,3]triazole	636.4 g	143.08CNY/2.5 kg, Adamas	36.4/5
(bromomethyl)cyclohexane	1.14 kg	666CNY/500 g, Adamas	1518.5/209.6
t-BuOK	653.4 g	303.68CNY/2.5 kg, Adamas	79.4/11
Bu_4BrN	32 g	35.04CNY/500 g, Adamas	2.2/0.3
MeOH	9 L	90CNY/4 L, Adamas	202.5/27.9
3-hexylthiophene (847.9 g)			
3-bromothiophene	1.10 kg	336CNY/500 g, Adamas	739.2/102
1-bromohexane	1.44 kg	463.54CNY/2.5 kg, Adamas	267/36.9
Mg	233.5 g	125CNY/25 g	1167.5/161.1
I_2	276 grains	857.75CNY/100 g, Adamas	857.8/118.4
$Ni(dppp)Cl_2$	72.9 g	529CNY/500 g, Adamas	77/10.6
2FIC	463.5 g		13882/1916
Total cost for 1 kg BZ4F-ch1			32647.2/4506.4
Total cost for 1 g BZ4F-ch1			32.6/4.5

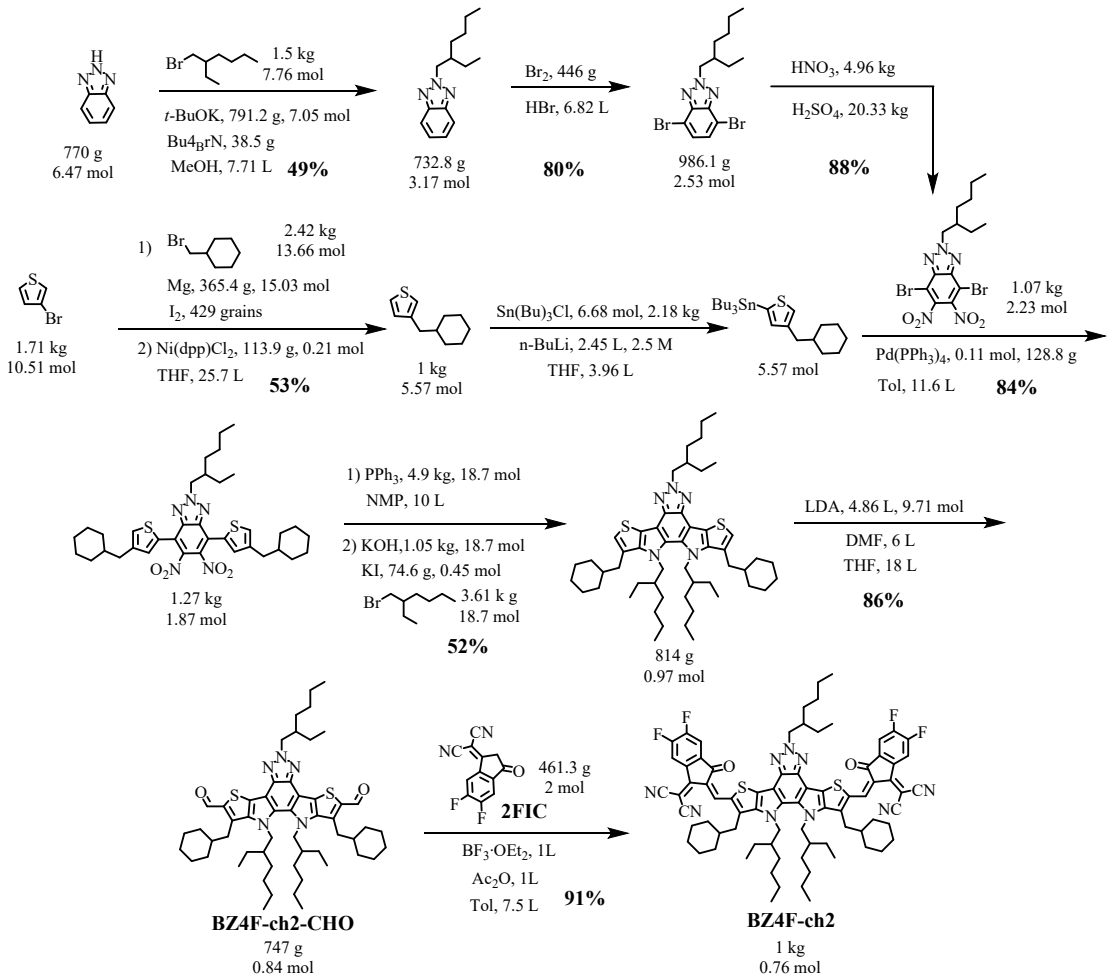

Scheme S4. The detailed synthetic route and the yield of each step of BZ4F-ch2.

Table S8. The MOC (material only cost) evaluation of BZ4F-ch2.

BZ4F-ch2-CHO (747 g)			
Reagent	Quantity	Unit price	Cost (CNY/dollar)
toluene	19.1 L	315CNY/10 L, Greagent	601.7/83
BF_3 OEt_3	1 L	680.11CNY/2.5 L, Aladdin	272/37.5
AC_2O	1 L	60CNY/500 mL, Greagent	120/16.6
LDA	4.86 L	230CNY/1 L, Energy Chemical	1117.8/154.3
THF	47.66 L	1200CNY/16 L, Energy Chemical	3574.5/493.3

DMF	6 L	950CNY/25 L, Energy Chemical	228/31.5
NMP	10 L	1795CNY/16 L, Adamas	1121.9/154.8
PPh_3	4.9 kg	2589CNY/25 kg, Energy Chemical	507.4/70
KOH	1.05 kg	28CNY/500 g, Energy Chemical	58.8/8.1
KI	74.6 g	65CNY/100 g, Adamas	48.5/6.7
1-bromo-2-ethylhexane	3.61 kg	304CNY/2.5 kg, Adamas	439/60.6
$Pd(PPh_3)_4$	128.8 g	3495CNY/100 g, Adamas	4501.6/621.2
n-BuLi	2.45 L	290CNY/1 L, Energy Chemical	710.5/98
$Sn(Bu)_3Cl$	2.18 kg	946.33CNY/2.5 kg, Adamas	825.2/113.9
3-bromothiophene	1.71 kg	336CNY/500 g, Adamas	1149.1/158.6
(bromomethyl)cyclohexane	2.42 kg	666CNY/500 g, Adamas	3223.4/444.8
Mg	365.4 g	125CNY/25 g	1827/252.1
I_2	429 grains	857.75CNY/100 g, Adamas	857.8/118.4
$Ni(dppp)Cl_2$	113.9 g	529CNY/500 g, Adamas	120.5/16.6
Compound 10 (1.07 kg)			
HNO_3	4.96 kg	500CNY/25 kg, Greagent	99.2/13.7
H_2SO_4	20.33 kg	350CNY/25 kg, Greagent	284.6/39.3
HBr	6.82 L	169.4CNY/2.5 L, Adamas	462.1/63.8
Br_2	446 g	220CNY/500 g, Chron Chemicals	196.2/27.1
2H-benzo[d][1,2,3]triazole	770 g	143.08CNY/2.5 kg, Adamas	44.1/6.1
1-bromo-2-ethylhexane	1.5 kg	304CNY/2.5 kg,	182.4/25.2

		Adamas	
t-BuOK	791.2 g	303.68CNY/2.5 kg, Adamas	96.1/13.3
Bu_4BrN	38.5 g	35.04CNY/500 g, Adamas	2.7/0.4
MeOH	7.71 L	90CNY/4 L, Adamas	173.5/23.9
2FIC	461.3 g		13816/1906.9
Total cost for 1 kg BZ4F-ch2			36662/5060
Total cost for 1 g BZ4F-ch2			36.7/5.1

Table S9. The MOC (material only cost) of small molecule acceptors.

Acceptors	PCE (%)	MOC ($/g)	PCE/MOC	Ref.
TBT13	16.1	11	1.46	[28]
IT-4F	13.7	16	0.86	[28-29]
BTP-eC9	18.87	19	0.99	[28, 30]
DF-PCIC	10.14	43	0.24	[28, 31]
2BTh-2F	15.44	21	0.74	[28, 32]
A4T-16	15.2	20	0.76	[28, 33]
PTIC	10.3	22	0.47	[28, 34]
Y6	18.2	25.68	0.71	[7, 35-36]
TBT-2	13.6	11.5	1.18	[35, 37]
TBT-9	7.18	9.18	0.78	[35]
TBT-26	17.0	12	1.42	[35]
BZ4F-ch1	16.02	4.5	3.56	This work
BZ4F-ch2	15.04	5.1	2.95	This work

References

1. Song, J.; Cai, F.; Zhu, C.; Chen, H.; Wei, Q.; Li, D.; Zhang, C.; Zhang, R.; CNY, J.; Peng, H.; So, S. K.; Zou, Y., Over 13% Efficient Organic Solar Cells Based on Low-Cost Pentacyclic A-DA′D-A-Type Nonfullerene Acceptor. *Solar RRL* **2021,** *5* (8), 2100281.

2. Feng, L.; CNY, J.; Zhang, Z.; Peng, H.; Zhang, Z.-G.; Xu, S.; Liu, Y.; Li, Y.; Zou,

Y., Thieno[3,2-b]pyrrolo-Fused Pentacyclic Benzotriazole-Based Acceptor for Efficient Organic Photovoltaics. *ACS Applied Materials & Interfaces* **2017,** *9* (37), 31985-31992.

3. Wei, Q.; Liang, S.; Liu, W.; Hu, Y.; Qiu, B.; Ren, J.; CNY, J.; Huang, F.; Zou, Y.; Li, Y., Effects of Oxygen Position in the Alkoxy Substituents on the Photovoltaic Performance of A-DA′D-A Type Pentacyclic Small Molecule Acceptors. *ACS Energy Letters* **2022,** *7* (7), 2373-2381.

4. Zhu, S.; Shi, C.; Wei, Q.; Zhu, C.; Ren, J.; Li, J.; Meng, L.; Li, Y.; CNY, J.; Zou, Y., A-DA'D-A Type Pentacyclic Small Molecule Acceptors to Exceed 16.5% Efficiency by Heteroatom Effect at the Outer Side Chain. *Chinese Journal of Chemistry* **2023,** *41* (15), 1815-1822.

5. Wang, Z.; Wei, W.; Zeng, L.; Liu, T.; CNY, X.; Zhou, J.; Yin, B.; Li, J.; Xie, Z.; Huang, F.; Cao, Y.; Duan, C., A–DA′D–A-Type Pentacyclic Fused-Ring Electron Acceptors for Efficient Organic Solar Cells. *Chemistry of Materials* **2023,** *35* (17), 6932-6942.

6. CNY, J.; Zhang, Y.; Zhou, L.; Zhang, C.; Lau, T. K.; Zhang, G.; Lu, X.; Yip, H. L.; So, S. K.; Beaupre, S.; Mainville, M.; Johnson, P. A.; Leclerc, M.; Chen, H.; Peng, H.; Li, Y.; Zou, Y., Fused Benzothiadiazole: A Building Block for n-Type Organic Acceptor to Achieve High-Performance Organic Solar Cells. *Adv Mater* **2019,** *31* (17), e1807577.

7. CNY, J.; Zhang, Y.; Zhou, L.; Zhang, G.; Yip, H.-L.; Lau, T.-K.; Lu, X.; Zhu, C.; Peng, H.; Johnson, P. A.; Leclerc, M.; Cao, Y.; Ulanski, J.; Li, Y.; Zou, Y., Single-Junction Organic Solar Cell with over 15% Efficiency Using Fused-Ring Acceptor with Electron-Deficient Core. *Joule* **2019,** *3* (4), 1140-1151.

8. CNY, J.; Huang, T.; Cheng, P.; Zou, Y.; Zhang, H.; Yang, J. L.; Chang, S. Y.; Zhang, Z.; Huang, W.; Wang, R.; Meng, D.; Gao, F.; Yang, Y., Enabling low voltage losses and high photocurrent in fullerene-free organic photovoltaics. *Nat Commun* **2019,** *10* (1), 570.

9. Li, C.; Zhou, J.; Song, J.; Xu, J.; Zhang, H.; Zhang, X.; Guo, J.; Zhu, L.; Wei, D.; Han, G.; Min, J.; Zhang, Y.; Xie, Z.; Yi, Y.; Yan, H.; Gao, F.; Liu, F.; Sun, Y., Non-

fullerene acceptors with branched side chains and improved molecular packing to exceed 18% efficiency in organic solar cells. *Nature Energy* **2021,** *6* (6), 605-613.

10. Mo, D.; Chen, H.; Zhu, Y.; Huang, H. H.; Chao, P.; He, F., Effects of Halogenated End Groups on the Performance of Nonfullerene Acceptors. *ACS Appl Mater Interfaces* **2021,** *13* (5), 6147-6155.

11. Chen, Y. Z.; Bai, F. J.; Peng, Z. X.; Zhu, L.; Zhang, J. Q.; Zou, X. H.; Qin, Y. P.; Kim, H.; CNY, J.; Ma, L. K.; Zhang, J.; Yu, H.; Chow, P. C. Y.; Huang, F.; Zou, Y. P.; Ade, H.; Liu, F.; Yan, H., Asymmetric Alkoxy and Alkyl Substitution on Nonfullerene Acceptors Enabling High-Performance Organic Solar Cells. *Advanced Energy Materials* **2021,** *11* (3), 2003141.

12. Yu, H.; Qi, Z.; Zhang, J.; Wang, Z.; Sun, R.; Chang, Y.; Sun, H.; Zhou, W.; Min, J.; Ade, H.; Yan, H., Tailoring non-fullerene acceptors using selenium-incorporated heterocycles for organic solar cells with over 16% efficiency. *Journal of Materials Chemistry A* **2020,** *8* (45), 23756-23765.

13. Lin, Y.; He, Q.; Zhao, F.; Huo, L.; Mai, J.; Lu, X.; Su, C.-J.; Li, T.; Wang, J.; Zhu, J.; Sun, Y.; Wang, C.; Zhan, X., A Facile Planar Fused-Ring Electron Acceptor for As-Cast Polymer Solar Cells with 8.71% Efficiency. *J. Am. Chem. Soc.* **2016,** *138* (9), 2973-2976.

14. Lin, Y.; Li, T.; Zhao, F.; Han, L.; Wang, Z.; Wu, Y.; He, Q.; Wang, J.; Huo, L.; Sun, Y.; Wang, C.; Ma, W.; Zhan, X., Structure Evolution of Oligomer Fused-Ring Electron Acceptors toward High Efficiency of As-Cast Polymer Solar Cells. *Advanced Energy Materials* **2016,** *6* (18), 1600854.

15. Li, R.; Liu, G.; Xiao, M.; Yang, X.; Liu, X.; Wang, Z.; Ying, L.; Huang, F.; Cao, Y., Non-fullerene acceptors based on fused-ring oligomers for efficient polymer solar cells via complementary light-absorption. *Journal of Materials Chemistry A* **2017,** *5* (45), 23926-23936.

16. Li, S.; Ye, L.; Zhao, W.; Liu, X.; Zhu, J.; Ade, H.; Hou, J., Design of a New Small-Molecule Electron Acceptor Enables Efficient Polymer Solar Cells with High Fill Factor. *Adv Mater* **2017,** *29* (46), 1704051.

17. Wu, H.; Fan, H.; Xu, S.; Zhang, C.; Chen, S.; Yang, C.; Chen, D.; Liu, F.; Zhu,

X., A Designed Ladder-Type Heteroarene Benzodi(Thienopyran) for High-Performance Fullerene-Free Organic Solar Cells. *Solar RRL* **2017,** *1* (12), 1700165.

18. Li, R.; Liu, G.; Xie, R.; Wang, Z.; Yang, X.; An, K.; Zhong, W.; Jiang, X.-F.; Ying, L.; Huang, F.; Cao, Y., Introducing cyclic alkyl chains into small-molecule acceptors for efficient polymer solar cells. *J. Mater. Chem. C* **2018,** *6* (26), 7046-7053.

19. Lin, Y.; Zhao, F.; Prasad, S. K. K.; Chen, J. D.; Cai, W.; Zhang, Q.; Chen, K.; Wu, Y.; Ma, W.; Gao, F.; Tang, J. X.; Wang, C.; You, W.; Hodgkiss, J. M.; Zhan, X., Balanced Partnership between Donor and Acceptor Components in Nonfullerene Organic Solar Cells with >12% Efficiency. *Adv Mater* **2018,** *30* (16), e1706363.

20. Luo, Z.; Sun, C.; Chen, S.; Zhang, Z.-G.; Wu, K.; Qiu, B.; Yang, C.; Li, Y.; Yang, C., Side-Chain Impact on Molecular Orientation of Organic Semiconductor Acceptors: High Performance Nonfullerene Polymer Solar Cells with Thick Active Layer over 400 nm. *Advanced Energy Materials* **2018,** *8* (23), 1800856.

21. Qu, J.; Chen, H.; Zhou, J.; Lai, H.; Liu, T.; Chao, P.; Li, D.; Xie, Z.; He, F.; Ma, Y., Chlorine Atom-Induced Molecular Interlocked Network in a Non-Fullerene Acceptor. *ACS Appl Mater Interfaces* **2018,** *10* (46), 39992-40000.

22. Zhu, J.; Wu, Y.; Rech, J.; Wang, J.; Liu, K.; Li, T.; Lin, Y.; Ma, W.; You, W.; Zhan, X., Enhancing the performance of a fused-ring electron acceptor via extending benzene to naphthalene. *J. Mater. Chem. C* **2018,** *6* (1), 66-71.

23. Wu, H.; Yue, Q.; Zhou, Z.; Chen, S.; Zhang, D.; Xu, S.; Zhou, H.; Yang, C.; Fan, H.; Zhu, X., Cathode interfacial layer-free all small-molecule solar cells with efficiency over 12%. *Journal of Materials Chemistry A* **2019,** *7* (26), 15944-15950.

24. Chen, X.; Liu, H.; Xia, L.; Hayat, T.; Alsaedi, A.; Tan, Z., A pentacyclic S,N-heteroacene based electron acceptor with strong near-infrared absorption for efficient organic solar cells. *Chem Commun (Camb)* **2019,** *55* (49), 7057-7060.

25. Li, X.; Pan, F.; Sun, C.; Zhang, M.; Wang, Z.; Du, J.; Wang, J.; Xiao, M.; Xue, L.; Zhang, Z. G.; Zhang, C.; Liu, F.; Li, Y., Simplified synthetic routes for low cost and high photovoltaic performance n-type organic semiconductor acceptors. *Nat Commun* **2019,** *10* (1), 519.

26. Li, Y.; Zheng, N.; Yu, L.; Wen, S.; Gao, C.; Sun, M.; Yang, R., A Simple Phenyl

Group Introduced at the Tail of Alkyl Side Chains of Small Molecular Acceptors: New Strategy to Balance the Crystallinity of Acceptors and Miscibility of Bulk Heterojunction Enabling Highly Efficient Organic Solar Cells. *Advanced Materials* **2019,** *31* (12), 1807832.

27. Wei, W.; CNY, X.; Zhong, J.; Wang, Z.; Zhou, X.; Zhao, F.; Feng, D.; Zhang, Y.; Chen, W.; Yang, M.; Zhang, W.; Ma, Z.; Tang, Z.; Lu, X.; Huang, F.; Cao, Y.; Duan, C., High-efficiency organic solar cells from low-cost pentacyclic fused-ring electron acceptors via crystal engineering. *Energy & Environmental Science* **2024,** DOI: 10.1039/d4ee02296c.

28. Yang, N.; Cui, Y.; Zhang, T.; An, C. B.; Chen, Z. H.; Xiao, Y.; Yu, Y.; Wang, Y. F.; Hao, X. T.; Hou, J. H., Molecular Design of Fully Nonfused Acceptors for Efficient Organic Photovoltaic Cells. *J. Am. Chem. Soc.* **2024,** *146* (13), 9205-9215.

29. Li, W.; Ye, L.; Li, S.; Yao, H.; Ade, H.; Hou, J., A High-Efficiency Organic Solar Cell Enabled by the Strong Intramolecular Electron Push-Pull Effect of the Nonfullerene Acceptor. *Adv Mater* **2018,** *30* (16), e1707170.

30. Fu, J.; Yang, Q.; Huang, P.; Chung, S.; Cho, K.; Kan, Z.; Liu, H.; Lu, X.; Lang, Y.; Lai, H.; He, F.; Fong, P. W. K.; Lu, S.; Yang, Y.; Xiao, Z.; Li, G., Rational molecular and device design enables organic solar cells approaching 20% efficiency. *Nature Communications* **2024,** *15* (1), 1830.

31. Li, S.; Zhan, L.; Liu, F.; Ren, J.; Shi, M.; Li, C. Z.; Russell, T. P.; Chen, H., An Unfused-Core-Based Nonfullerene Acceptor Enables High-Efficiency Organic Solar Cells with Excellent Morphological Stability at High Temperatures. *Advanced Materials* **2017,** *30* (6), 1705208.

32. Wang, X.; Lu, H.; Liu, Y.; Zhang, A.; Yu, N.; Wang, H.; Li, S.; Zhou, Y.; Xu, X.; Tang, Z.; Bo, Z., Simple Nonfused Ring Electron Acceptors with 3D Network Packing Structure Boosting the Efficiency of Organic Solar Cells to 15.44%. *Advanced Energy Materials* **2021,** *11* (45), 2102591.

33. Ma, L.; Zhang, S.; Zhu, J.; Wang, J.; Ren, J.; Zhang, J.; Hou, J., Completely non-fused electron acceptor with 3D-interpenetrated crystalline structure enables efficient and stable organic solar cell. *Nature Communications* **2021,** *12* (1), 5093.

34. Yu, Z. P.; Liu, Z. X.; Chen, F. X.; Qin, R.; Lau, T. K.; Yin, J. L.; Kong, X.; Lu, X.; Shi, M.; Li, C. Z.; Chen, H., Simple non-fused electron acceptors for efficient and stable organic solar cells. *Nat Commun* **2019,** *10* (1), 2152.

35. Yang, N.; Cui, Y.; Xiao, Y.; Chen, Z. H.; Zhang, T.; Yu, Y.; Ren, J. Z.; Wang, W. X.; Ma, L. J.; Hou, J. H., Completely Non-Fused Low-Cost Acceptor Enables Organic Photovoltaic Cells with 17 % Efficiency. *Angew. Chem.-Int. Edit.* **2024**, e202403753

36. Liu, Q.; Jiang, Y.; Jin, K.; Qin, J.; Xu, J.; Li, W.; Xiong, J.; Liu, J.; Xiao, Z.; Sun, K.; Yang, S.; Zhang, X.; Ding, L., 18% Efficiency organic solar cells. *Science Bulletin* **2020,** *65* (4), 272-275.

37. Yang, N.; Zhang, T.; Wang, S. J.; An, C. B.; Seibt, S.; Wang, G. L.; Wang, J. W.; Yang, Y.; Wang, W. X.; Xiao, Y.; Yao, H. F.; Zhang, S. Q.; Ma, W.; Hou, J. H., An Ortho-Bisalkyloxylated Benzene-Based Fully Non-fused Electron Acceptor for Efficient Organic Photovoltaic Cells. *Small Methods* **2024,** *8* (2), 2300036.